

Squirrels (Rodentia, Sciuridae) of the Early Miocene Tagay fauna in Eastern Siberia

Maxim Sinitsa^{1,2,3} and Alexey Tesakov⁴

¹Ural Federal University, ul. Mira, 19, Ekaterinburg, 620002, Russian Federation

²Università Roma Tre, Largo S. L. Murialdo, 1, Rome, 00146, Italy

³Borissiak Paleontological Institute, Russian Academy of Sciences, ul. Profsoyuznaya, 123, Moscow, 117997, Russian Federation

⁴Geological Institute, Russian Academy of Sciences, Pyzhevskiy per., 7, Moscow, 119017, Russian Federation

Address correspondence and requests for materials to Alexey Tesakov, tesak@ginras.ru, tesak-ov@yandex.ru

Abstract

The Tagay vertebrate fauna (Olkhon Island, Lake Baikal, Russia) dated to the late Early Miocene yielded a diverse association of sciurine rodents, including flying squirrel *Hylopetes* sp., tree squirrels *Sciurus* cf. *lii*, *Sciurus* sp., and *Blackia* cf. *miocae-nica*, and a numerically dominant small marmotine *Miospermophilus debruijini*. The presence of flying and tree squirrels indicates the presence of wooded biotopes. The record of *Blackia* is remarkably distant (more than 4000 km) from the nearest synchronous records in western Asia (Anatolia) and Eastern Europe thus implying a continuous distribution range of this genus stretching through the middle latitudes of the Holarctic and likely marking the continental belt of temperate forests in late Early Miocene. Marmotines of North American origin document direct faunal communication between temperate faunas of the Old and New Worlds at that time.

Keywords: Mammalia, squirrels, *Blackia*, *Hylopetes*, *Miospermophilus*, *Sciurus*, Early Miocene, Baikal, Olkhon, Russia

Introduction

The Miocene Tagay fauna from Olkhon Island of Lake Baikal is one of the few vertebrate faunas of this age known from the vast Eastern Siberia. It is also the northernmost fauna that records a Miocene mesic biota of the temperate forest zone beyond the well-studied more arid settings of Mongolia, North China, and Kazakhstan. Known since the mid 20th century, the Tagay locality has been variably dated in the range from Early Miocene (Vislobokova, 1994, 2004), late Middle Miocene (Daxner-Höck et al., 2013) to Middle-Late Miocene (Logatchev, Lomonosova, and Klimanova, 1964; Pokatilov, 2012). Most recent contributions based on mammalian fauna and paleomagnetic data estimate the age of the fauna as late Early Miocene, Shanwangian ALMA, MN5 (Tesakov and Lopatin, 2015; Sotnikova, Klementiev, Sizov, and Tesakov, 2021; Daxner-Höck et al., 2022a). A magnetostratigraphic correlation of this sequence to paleomagnetic chrons C5Dn through C5Cn.1n in the range of ca. 17.2 to 16.2 Ma (Burdigalian) (Kazansky et al., 2022) though seems to be unrealistically long for a very uniform fauna of Tagay.

The vertebrate fauna of Tagay has been mentioned in numerous recent publications devoted to herpetofauna (Rage and Danilov, 2008; Syromyatnikova, 2016; and others), birds (Zelenkov, 2016; Volkova and Zelenkov, 2018; Volkova, 2020; and others) and mammals (Klementiev and Sizov, 2015; Tesakov and Lopatin, 2015; Sotnikova et al., 2021; Daxner-Höck et al., 2022a and references herein; Sizov, Klementiev, and Pierre-Olivier, 2023).

The Tagay Miocene site is associated with extensive, distinctly bedded deposits of alternating sandy-clayey and calcareous beds with an overall thickness of up to 15 m. The section is located on the western shore of Olkhon Island in Tagay Bay (N 53.16040° E 107.21154°). The site formed in a shallow water lacustrine basin

Citation: Sinitsa, M. and Tesakov, A. 2023. Squirrels (Rodentia, Sciuridae) of the Early Miocene Tagay fauna in Eastern Siberia. *Bio. Comm.* 68(4): 273–290. <https://doi.org/10.21638/spbu03.2023.407>

Authors' information: Maxim Sinitsa, PhD, Associate Professor, orcid.org/0000-0001-6814-4324; Alexey Tesakov, Dr. of Sci. in Geology and Mineralogy, Head of Laboratory, orcid.org/0000-0002-8616-2291

Manuscript Editor: Pavel Skutschas, Department of Vertebrate Zoology, Faculty of Biology, Saint Petersburg State University, Saint Petersburg, Russia

Received: September 20, 2023;

Revised: October 29, 2023;

Accepted: November 2, 2023.

Copyright: © 2023 Sinitsa and Tesakov. This is an open-access article distributed under the terms of the License Agreement with Saint Petersburg State University, which permits to the authors unrestricted distribution, and self-archiving free of charge.

Funding: The research was supported by the project of the Russian Science Foundation, no. 23-24-00267.

Ethics statement: This paper does not contain any studies involving human participants or animals performed by any of the authors.

Competing interests: The authors have declared that no competing interests exist.

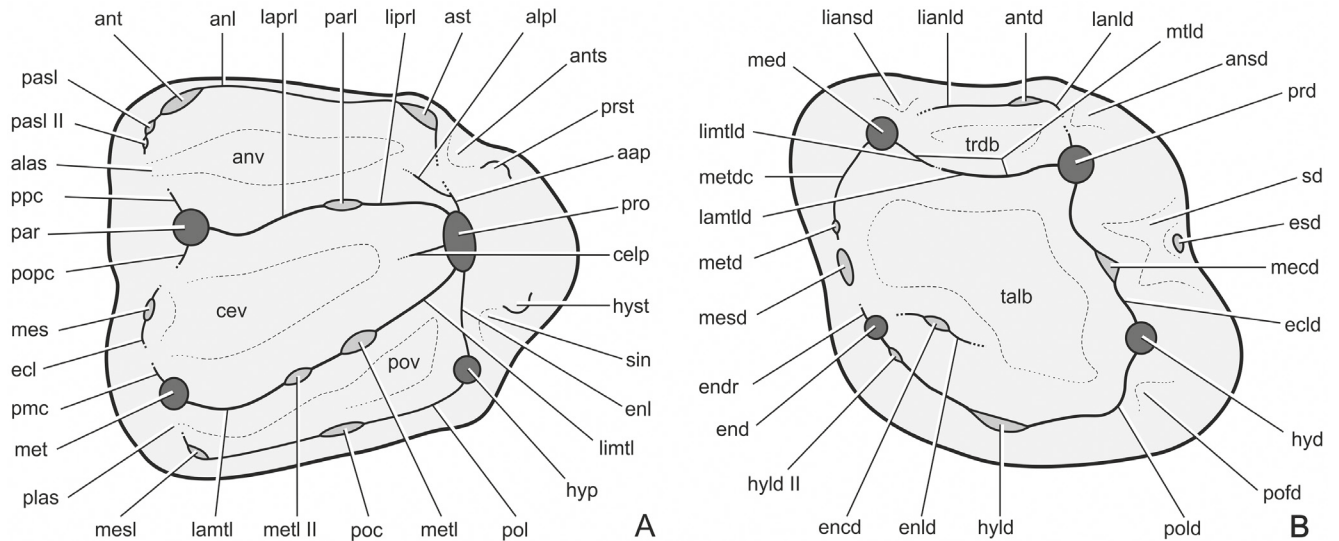


Fig. 1. Right side upper (A) and lower (B) sciurid cheek teeth illustrating the terminology used. Abbreviations: aap — anterior arm of protocone; alas — anterolabial sinus; alpl — anterolophule; ancd — anterior cingulid; anl — anteroloph; anld — anterolophid; ansd — anterosingulid; ant — anterocone; ants — antesinus; ast — anterostyle; antd — anteroconulid; anv — anterior valley; celp — centrolophule; cev — central valley; ecl — ectoloph; ecld — ectolophid; encd — entoconulid; end — entoconid; endr — entoconid ridge; enl — endoloph; enld — entolophid; hyst — hypostyle; lamtl — labial metaloph; lamtld — labial metalophid; lanld — labial anterolophid; laprl — labial protoloph; lianld — lingual anterolophid; liansd — lingual anterosingulid; limtl — lingual metaloph; limtld — lingual metalophid; liprl — lingual protoloph; mecd — mesoconid; med — metaconid; mes — mesostyle; mesd — mesostylid; mesl — metastyle; met — metacone; metd — metastylid; metdc — metastylid crest; metl — metaconule; metl II — metaconule II (second metaconule); mtld — metalophid; par — paracone; parl — paraconule; pasl — parastyle; pasl II — parastyle II (second parastyle); plas — posterolabial sinus; pmc — premetacrista; poc — posterocone; pofd — postflexid; pol — posteroloph; pold — posterolophid; popc — postparacrista; pov — posterior valley; ppc — preparacrista; prd — protoconid; pro — protocone; prst — protostyle; sd — sinusid; sin — sinus; talb — talonid basin; trdb — trigonid basin.

under warm temperate conditions with humid and semi-arid climatic phases (Sizov and Klementiev, 2015). Eight superposed fossiliferous beds (labeled downsection as A–H) produced a nearly identical taxonomic list of small mammals thus indicating a rapid sedimentation rate.

Smaller squirrels of Tagay were reported as *Sciuridae* gen. et sp. by Daxner-Höck et al. (2013) and *Spermophilus debruijini* sp. nov. (Daxner-Höck et al., 2022b).

Our excavations of 2008–2020 yielded extensive small mammal material. In this contribution, we revise the taxonomic position of previously described sciurids and provide a detailed description of squirrels from Tagay based on the new material.

Material and methods

All described materials were collected during several field sampling campaigns, especially those supported by the project of the Russian Foundation for basic research, no. 14-04-00575, Neogene vertebrates of the Cis-Baikal region as a key to the understanding of land biota evolution in Northern Eurasia.

The remains of *Sciuridae* were extracted from fossiliferous deposits in the field by manual and water-pump wet screening with a mesh size of 0.5–0.7 mm. The dried bone-bearing concentrate was separated into size fractions and manually sorted in the field and in the laboratory. The material described in this paper originated

from the fossiliferous bed E in the middle part of the sequence (Sizov and Klementiev, 2015; Sizov, Klementiev, and Pierre-Olivier, 2023).

The photographic images of dental specimens were taken from ammonium chloride-coated high-resolution resin casts using Canon MP-E 65 mm macro lens with an APS-C DSLR camera.

The described material is stored in the Geological Institute of the Russian Academy of Sciences in Moscow (GIN), under collection number GIN 1138.

The terminology of sciurid dental elements (Fig. 1) is after Sinitsa (2018) and Sinitsa and Pogodina (2019). Measurements were taken, as defined by van de Weerd (1976), using the ocular micrometer of the binocular microscope calibrated against the reference scale. Upper case D, P, M denote upper row deciduous, premolar, and molar teeth; lower case d, p, m, = lower row deciduous, premolar, and molar teeth.

The classification of *Sciuridae* follows Stepan et al. (2004) and Thorington and Hoffmann (2005). Subtribal- and generic-level systematics of *Marmotini* follow Sinitsa (2018) and Sinitsa, Čermák, and Kryuchkova (2022).

Systematic paleontology

Order Rodentia Bowdich, 1821
 Family Sciuridae Fischer, 1817
 Subfamily Sciurinae Fischer, 1817
 Tribe Sciurini Fisher, 1817

Genus *Sciurus* Linnaeus, 1758

Sciurus cf. *lii* Qiu and Yan, 2005

Fig. 2A–F

Materials — GIN 1138/146, right M2; GIN 1138/184, left M3; GIN 1138/185, left m2; GIN 1138/177, 186, 187, left m3.

Description — The M2 is roundly trapezoidal in occlusal outline with a laterally expanded posterolabial portion (L–2.65, W–3.15 mm; Fig. 2A). The posterior and anterior sides of the crown are straightened; lingually, the crown is rounded. The anteroloph is a simple and even ridge that completely encloses the anterior valley. The lingual arm of the ridge at the contact with protocone protrudes medially and forms a shallow antesinus depression just anterior to the cusp. The protocone, which dominates the crown, is massive and transversely compressed. The cusp is connected to a lophate and laterally shifted hypocone via a stout endoloph. The paracone and metacone are well-developed, although partially submerged into the main loph. The protoloph is nearly transversal with a slight paraconule swelling on its lingual half. The metaloph is oriented slightly anterolingually towards the posterior wall of the protoloph and shows no traits of metacornules or constrictions at contact with the metacone. The ridges are complete and oriented towards the anterior and posterior edges of the protocone respectively. The central valley is expansive, about two times longer anteroposteriorly than the anterior valley, and five times longer than the posterior one. The enamel surface in these basins is slightly rugose. Approximately halfway between the paracone and metacone is a prominent mesostyle that is connected to the paracone by a thin posparacrista. A minute second mesostyle is present immediately posterior to the main cuspid. Lingually to them, the bottom of the central valley is complicated by a knoblike irregular cuspid, comparable in size to the second mesostyle. The posteroloph is well-developed and complete with no indication of accessory cusps.

Among the specimens from Tagay attributable to a medium-sized species of the genus *Sciurus*, is a rounded and slightly weathered M3 of an adult individual (L–2.80, W–2.81 mm; Fig. 2B). The crown is roundly triangular in occlusal outline. The posterior lobe is massive and expansive so that its lateralmost edge is set labial to the paracone. The anteroloph is a gentle arc along the entire anterior side of the crown. The loph is devoid of cuspid and seamlessly fused with the anterior side of the protocone; the labial end appears to fade out before reaching the paracone, thus leaving the anterior valley open. A shallow, albeit broad, toque-like anterolophule extends from the labial side of the lingual arm of the anteroloph towards the central part of the anterior valley. The protocone is a transversally compressed lophate cusp that continues posteriorly by an endoloph and posteroloph, with no indication of a hypocone. A pointed

and slightly anteroposteriorly compressed paracone is taller than the protocone and dominates the crown. The protoloph arises from the anterolabial side of the protocone to fuse with the paracone. The ridge is straight, even, and widens labially. Immediately posterior to the lingual arm of the protoloph is a well-defined protolophule, similar in shape to the anterolophule. The central and posterior valleys are fused, forming a vast and smoothly rugose posterior basin. The basin is rimmed by a low posteroloph.

The m2 is rhomboid in occlusal outline (Fig. 2C), wider than long, and its trigonid part is slightly wider on average than the talonid one, although the difference is slight (L–2.81, W–3.18 mm). The four main cusps are well-developed with the trigonid pair being only slightly taller than the talonid cusps. The most pronounced of the transverse crests are the anterolophid and the labial metalophid, which together form a characteristic Y-shaped lophid. A recessed trigonid basin is wedged between the lophids and closed labially by a thin extension of the labial end of the anterolophid, which hooks backwards to contact the anterior arm of the protoconid. The specimen shows a smooth anteroconulid swelling on the anterolabial end of the anterolophid. The ectolophid is a thin M-shaped ridge connecting the posterolingual wall of the protoconid and an anterolingual wall of the hypoconid. A salient mesoconid is present in the ectolophid midway between the cusps and separated from them by a deep sinusid. The labial side of the mesoconid is strongly extended to form a robust ectomesolophid that reaches the lateral margin of the crown. On the opposite, medial side of the crown, a well-developed mesostylid is present between the metaconid and entoconid. Anteriorly, the mesostylid is connected to the metaconid via a sharp metastylid crest. The entoconid is a distinct cusp that slightly exceeds a hypoconid in height. The posterior edge of the tooth is marked by a prominent posterolophid. The lophid appears to be featureless and equally thick along its whole extent. A slight constriction is discernible at the contact with the hypoconid where a shallow postflexid indents the posterolabial wall of the tooth. The trigonid basin is smooth apart from its posterolabial corner housing low, irregular lophuli, which extend from the hypoconid towards the center of the basin.

The m3 is the largest of the cheek teeth (GIN 1138/186: L–2.87, W–2.82 mm; GIN 1138/177: L–3.12, W–2.99 mm; GIN 1138/187: L–3.18, W–3.43 mm). Viewed occlusally, the crown has a roughly rectangular outline due to a widened talonid (Fig. 2D–F). The trigonid portion of the tooth is much the same as in the preceding molar, except that it possesses a thinner and shorter anterolophid, a rudimentary metastylid crest, and a weaker metalophid that does not reach the anterolophid. A small anteroconulid is observable in one (GIN 1138/186) of the three m3s (Fig. 2E). The area of the sinusid is reminiscent

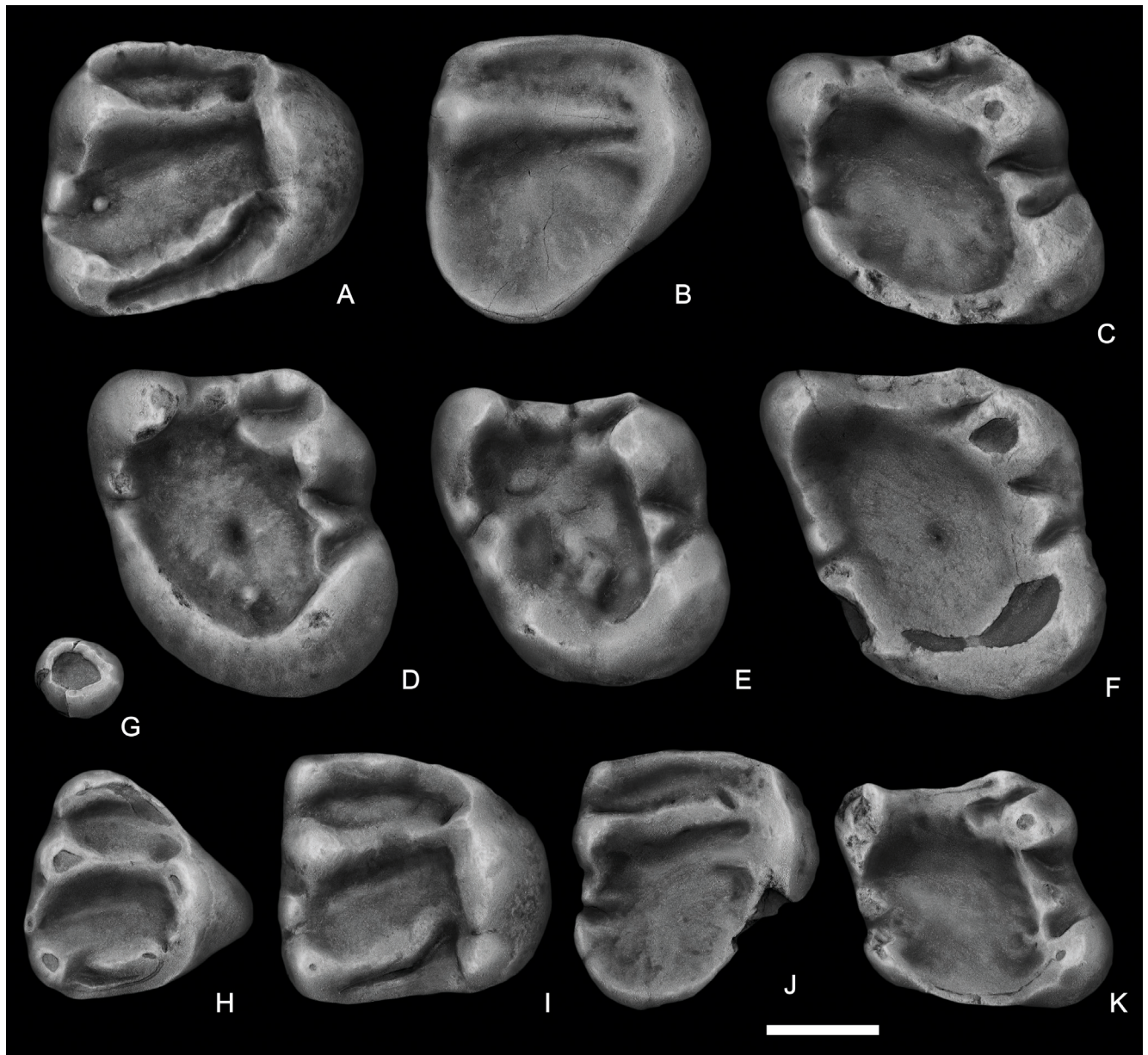


Fig. 2. *Sciurus cf. lii* Qiu and Yan, 2005 (A–F) and *Sciurus* sp. (G–L), Tagay; A, M2 (GIN 1138/146); B, M3 (GIN 1138/184); C, m2 (GIN 1138/185); D, m3 (GIN 1138/177); E, m3 (GIN 1138/186); F, m3 (GIN 1138/187); G, P3 (GIN 1138/149); H, DP4 (GIN 1138/182); I, M1 (GIN 1138/183); J, M3 (GIN 1138/181); K, m2 (GIN 1138/147). All teeth, except A and J are inverted. Scale bar equals 1 mm.

of the same structure in m2, with a complete, M-shaped ectolophid, and a prominent mesoconid forming a transversally directed ectomesolophid swelling. The mesostylid is notably smaller than in m2 and connected to the metaconid in one specimen only (GIN 1138/187; Fig. 2F). A well-developed posterolophid arcs from the hypoconid to the entoconid, defining a fairly rounded posterior margin of the tooth. An entoconid is present but partially submerged into the posterolophid and less distinct from this lophid than in the m2s. The enamel in the talonid basin is mostly smooth. There appears to be some irregularity of the enamel in the posterior part of the basin, nothing, however, could be interpreted as a distinct entoconulid or entolophid.

Comparisons and comments — The largest sciurid specimens from Tagay are the six molars described above. They represent a tree squirrel (Sciurinae) and are tentatively tentatively attributed here to *Sciurus lii* Qiu and Yan, 2005, based on the following combination of characters: medium-large size, comparable to *S. carolinensis*, *S. pucheranii*, *S. spadiceus*, and *S. variegatoides*, but larger than *S. aestuans*, *S. anomalus*, *S. aureogaster*, *S. deppei*, *S. granatensis*, *S. igniventris*, *S. lis*, *S. maltei*, *S. olsoni*, *S. vulgaris*, and *S. warthae* (Sulimski, 1964; Dahlmann, 2001), and smaller than *S. griseus*, *S. niger*, and large specimens of *S. variegatoides*; labially expanded posterior lobe of M3 with a remnant of the protolophule; the m2 and m3 with a tiny trigonid basin, strong mesoconid, and massive and

tall talonid portion, the enamel of the M3, m2, and m3 basins is uneven. *Sciurus lii* was named and described by Qiu and Yan (2005) on the basis of an incomplete skeleton preserving most of the teeth loci (except M1 and M2) from the late Early Miocene to early Middle Miocene diatomaceous lacustrine shales of the Shanwang locality in Shandong Province, China. No additional specimens have since been referred to this species, leaving a limited basis for the comparison of new material. We have not had the opportunity to study and compare the Shanwang holotype, but on the basis of the published illustrations (Qiu and Yan, 2005: fig. 2) and the measurements reported, the materials referred here seem not to differ substantially from it in any important respects. However, considering the combination of limited materials and some morphological differences (a more strongly irregular enamel of the talonid basins of m2 and m3, and the M3 with the anterolophule and stronger protolophule), we only refer it provisionally to *S. lii*, pending the discovery of new materials.

Sciurus sp.

Fig. 2G–K

Material — GIN 1138/149, right P3; GIN 1138/182, left DP4; GIN 1138/183, right M1; GIN 1138/181, left M3; GIN 1138/147, left m2.

Description — The P3 is a small tooth (L–0.77, W–0.87 mm), with a slightly elliptical occlusal outline (Fig. 2G). The most notable feature of the crown is a moderately excavated, rounded depression formed by fused central and posterior valleys, and rimmed by equally thickened protoloph and posteroloph. The lophs bear no cusps, except for a tiny circular cone at the labial protoloph–posteroloph junction, which we interpret as a remnant of paracone.

The DP4 is roughly triangular in occlusal outline (Fig. 2H), with flattened anterolingual and labial walls, and a rounded posterior wall (L–2.16, W–2.33 mm). The crown is dominated by pointed paracone and metacone lingually, and by the protocone lingually. The protocone and paracone are the tallest cusps. The anterior margin of the crown is defined by a stout anterocone, which reminds the major cusps in size. The cusps are separated by a vast central valley, a somewhat shorter anterior valley, and a small, anteroposteriorly narrowed posterior valley. The bottom of these valleys is smooth and featureless. A prominent anterior lobe of the tooth is rimmed by a voluminous anteroloph with two barely discernible cusps on it, an elliptical anterocone located close to the anteriormost point of the crest, and a low anterostyle, which forms a straight anterolingual wall of the anterior lobe. The antesisinus is closed by the anteroloph–protocone joint. The anterolabial sinus is a very narrow funnel. The paracone, as viewed occlusally, is triangular. It is connected to the protocone by a

low and transverse protoloph bearing a faint remnant of the paraconule on its lingual arm. The posterolabial wall of the paracone forms a pronounced and fairly straight postparacrista (posterior arm). The crest ends with a rounded mesostyle lying close to the metacone. The metacone is similar to the paracone in overall shape and size. The metaloph, in contrast to the protoloph, is thicker and constricted at the junction with metacone. A minute metaconule is discernible as a swelling on the lingual end of the ridge. Anterolingual to it, a massive endoloph forms a hypocone. The cusp is about one and a half times smaller than the protocone and partially fused to it anteriorly. The posterior end of the hypocone is continued into a thick and even posteroloph, which ends labially by a blunt metastyle swelling, thus leaving the posterior posterior valley open laterally.

In occlusal outline, the M1 is a rounded rectangle (L–2.43, W–2.71 mm), with nearly straight labial and posterior walls (Fig. 2I). The anterior lobe is wide labiolingually and anteroposteriorly elongated so that the anterior valley appears only slightly shorter than a vast central valley. A well-developed anteroloph runs along the entire anterior margin of the lobe from a salient anterocone and continues seamlessly into the anterior arm of the protocone. The lingual extent of the anteroloph is marked by a smooth anterostyle. A massive and blunt protocone is the tallest principal cusp followed by the paracone, metacone, and hypocone. The former is notably transversally compressed, whereas the rest are conical and rounded. Both protoloph and metaloph are complete, uninterrupted, decreased in width and height at their midlength, and devoid of paraconules and metaconules respectively. The bottom of the central sinus is occupied by a prominent mesostyle, which projects farther labially than the paracone and metacone. There is no ectoloph between the paracone and metacone. The posteroloph is a distinct, albeit low ridge extending labially from the hypocone to the metacone to enclose a rudimentary posterior valley.

In occlusal outline, the M3 is a rounded triangle (L–2.46, W–2.46 mm), with a large, posterolabially expanded posterior lobe (Fig. 2J). The crown lacks any signs of the metacone and most accessory cusps. The major cusps are barely discernible, especially the paracone and hypocone, which are completely submerged within the protoloph and endoloph respectively. The protocone is a thick lophate cusp that continues posteriorly by a massive endoloph and a posteroloph. The anterior arm of the protocone is thick and tapers anteriorly to fuse with a well-developed anteroloph. The anterolingual wall of the crown is gently depressed by a very shallow antesisinus. The anteroloph, which defines a sizeable anterior valley, is straightened and rather featureless with a small swelling at its labial end that represents an anterocone. There is a thick, albeit low, wedge-shaped anterolophule that

originates from the point where anteroloph joints the protocone and protrudes anterolabially into the anterior valley for about one-fifth of its width. The protoloph is straight, even, and oriented almost directly transversely and parallel to the anteroloph. The paracone thickening forms a short postparacrista and a weak preparacrista, which preserves the surface details nearly intact. A salient and thick protolophule, similar to the anterolophule in general appearance, is present at the anterolingual corner of the central valley. The ridge runs along the protoloph and fades out before reaching the mid-width of the valley. The posteroloph crosses the entire posterior edge of the crown and reaches the base of the metacone where forms a weak metastyle. The talon basin of the tooth along its posterior margin is filled with smooth irregular lophules extending from the posteroloph into the basin.

The m2 is slightly wider than long (L–2.30, W–2.64 mm). The posterolingual (entoconid) corner of the crown is well-developed, giving the crown a distinctly rectangular occlusal outline; the talonid portion of the crown is somewhat wider than the trigonid one (Fig. 2K). The crown is dominated by a tall metaconid; the remaining three principal cusps are almost equal in height. A voluminous anterolophid is complete from the metaconid to the anterolingual side of the protoconid. An anteroconulid swelling is observable in the labial extent of the ridge. A narrow and shallow trigonid basin confluent with anterosinusid separates the anteroconulid from the protoconid. The posterolingual rim of the trigonid basin is formed by a very short and irregular labial metalophid. The crest extends anteromedially to meet the labial one-third of the anterolophid. This results in a very small to almost non-existent trigonid basin. The labial cusps, namely the protoconid and hypoconid, are similar in size and slightly compressed anteroposteriorly. A straight ectolophid extends between the cusps to divide a sinus and rectangular talonid basin. The labial wall of the ridge expands outwards and forms a small well-developed mesoconid. Apart from a shallow postflexid, the posterior side of the crown is virtually featureless and represented by a thin arc of the posterolophid. A solid entoconid does not form the entoconid crest. A space between the entoconid and metaconid is occupied by a sharp metaconid crest and a large, fairly circular mesostylid. The enamel of the talonid basin is mostly smooth and tends to form a radially directed low lophuli associated with the inner walls of the anterolophid, ectolophid, hypoconid, and posterolophid.

Comparisons and comments — Among the specimens from Tagay attributable to the bushy-tailed squirrels, genus *Sciurus*, are five cheek teeth of small- to medium-sized species. Although morphologically similar, these specimens are substantially smaller than *Sciurus* cf. *lii* from Tagay and cannot be associated with this

form. In comparison with the extant species of the genus, the small-sized *Sciurus* from Tagay appears larger than *S. aestuans* and *S. igniventris*, smaller than *S. anomalus*, *S. aureogaster*, *S. carolinensis*, *S. griseus*, *S. niger*, *S. pucheranii*, *S. spadiceus*, *S. variegatoides*, *S. vulgaris*, and similar in size to *S. deppei*, *S. granatensis*, and *S. lis*. The presence of P3 distinguishes it from *S. aestuans*, *S. anomalus*, *S. aureogaster*, *S. granatensis*, *S. igniventris*, *S. niger*, *S. pucheranii*, and *S. spadiceus*. In terms of cheek teeth morphology, this form differs from most species of the genus in possessing the anterolophule and protolophule of M3 and a restricted trigonid basin of m2, and uneven basins of both upper and lower molars. The well-developed hypocone of M1 further differs it from *S. aestuans*, *S. anomalus*, *S. aureogaster*, *S. carolinensis*, *S. deppei*, *S. griseus*, *S. igniventris*, *S. niger*, *S. olsoni*, *S. vulgaris*, and *S. warthae*. This morphology is similar to that of *S. lii* and is likely plesiomorphic. Although the putative small-sized *Sciurus* from Tagay may represent morphological variability of *S. lii*, it appears substantially smaller than the former and shows stronger hypocone, not observable neither in the P4 from the type locality Shanwang nor in the M2 of *Sciurus* cf. *lii* described above. The small-sized bushy-tailed squirrel from Tagay likely represents a new species, most closely related to *S. lii*. However, naming is deferred until the extent of variability assessed with a larger sample is obtained.

Tribe Pteromyini Brandt, 1855

Genus *Hylopetes* Thomas, 1908

Hylopetes sp.

Fig. 3A–C

Material — GIN 1138/148, 176, left M1–2; GIN 1138/179, right M1–2; GIN 1138/145, right m1.

Description — The M1–2 has a rectangular occlusal outline with almost straight anterior, labial and posterior walls, and a rounded-angular lingual wall (L–1.57, W–1.79 mm; L–1.62, W–1.95 mm; L–1.75, W–1.81 mm; Fig. 3A, B). The latter is smoothly wrinkled and bears two major depressions, the antesisinus and sinus, which define the anterior and posterior edges of the protocone. The principal cusps, including the protocone, are weak and compressed. The lophs are rather high, straight, and separated by expansive valleys. The anterior valley is a large, fairly rectangular depression comparable in overall size to the central valley. The anterolabial edge of the anterior valley is marked by a pronounced anterocone. A thin anteroloph extends labially along the anterior edge of the valley and curves abruptly backwards toward the paracone. This longitudinal portion of the anteroloph is slightly swollen labially, suggesting a barely distinct anterolophule. The posterior edge of the anterior valley is delimited by a strong protoloph. The crest is gently arched posteriorly, nearly transversal in orientation, and strongly constricted at the contact with protocone. Labially, the

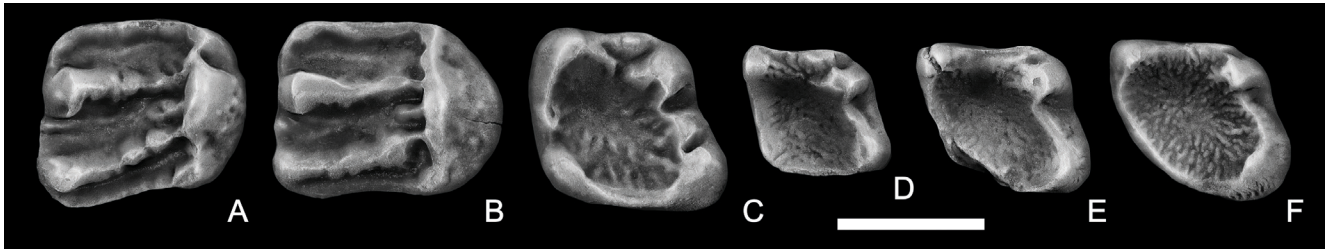


Fig. 3. *Hylopetes* sp. (A–C) and *Blackia* cf. *miocaenica* Mein, 1970 (D–F), Tagay; A, M1–2 (GIN 1138/179); B, M1–2 (GIN 1138/176); C, m1 (GIN 1138/145); D, m1 (GIN 1138/187); E, m2 (GIN 1138/188); F, m3 (GIN 1138/174). B, E, F — inverted. Scale bar equals 1 mm.

protoloph continues into the tall, albeit lophate, paracone with a short postparacrista. The anterior wall of the ridge is essentially smooth, whereas the posterior one is complicated by distinct undulating lophuli, which become obliterated with wear. In GIN 1138/148, there is a tiny paraconule on the lingual end of the protoloph. The metaloph is reminiscent of the protoloph in shape and size, being slightly narrower, lower, more inclined anterolingually, and having a well-developed metaconule. The metacone is almost submerged in the metaloph. The rectangular central valley is notable for two major structures, a transversal protolophule, and a knob-like mesostyle, which occasionally (GIN 1138/179) forms a prominent, lingually directed mesoloph (Fig. 3A). The posterior valley is about one and a half times anteroposteriorly shorter than the preceding depression. The lingual wall of the valley is formed by a strong, longitudinally oriented endoloph and a lateromedially compressed hypocone. The posteroloph is a weak, even, and low crest, about half the height of the hypocone in lightly worn specimens.

The only known m1 from Tagay is rectangular in occlusal view (L–1.75, W–1.81 mm); and slightly tapers anteriorly, being about 10% wider posteriorly (Fig. 3C). The metaconid is the tallest cusp. The remaining three major cusps, the protoconid, hypoconid, and entoconid appear to be similar in size and approximately half the height of the metaconid. The anterolophid is notably swollen but shortened and terminates without reaching the labial margin of the tooth. The metalophid is a blunt crest with an abrupt recession that divides it into a thicker labial metalophid and a thinner lingual metalophid. The latter contacts the lingual end of the anterolophid before reaching the base of the metaconid. A narrow ectolophid has a distinct M-shape configuration and bears a large mesoconid that is separated from the labial cusps by a deep sinusid. A pronounced metastylid crest extends directly posteriorly from the metaconid along the lingual wall of the tooth to contact with a strong mesostylid. The posterolophid is a simple crest that arcs along the entire posterior wall of the tooth and continues into the transversally compressed entoconid. The enamel surface in the talonid is wrinkled with irregular lophules which slope into the center of the basin.

Comparison and comments — The genus *Hylopetes* encompasses nine extant species of small- to medium-

sized flying squirrels distributed in southeastern tropical forests of Mainland Southeast Asia and the Malay Archipelago (Thorington and Hoffman, 2005; Thorington, Koprowski, Steele, and Whatton, 2012). Both morphological studies and the results of mitochondrial cytochrome b — based phylogenetic analyses suggest close relationships between *Hylopetes* a New World flying squirrel *Glaucomys*, and the dwarf flying squirrels, *Petinomys*, sympatric with *Hylopetes* (Thorington, Musante, Anderson, and Darrow, 1996; Thorington, Pitassy, and Jansa, 2002; Thorington, Koprowski, Steele, and Whatton, 2012; Rasmussen and Thorington, 2008; Fabre, Hautier, Dimitrov, and Douzery, 2012). In the realm of fossil record, *Hylopetes* represents a classical waste-basket taxon accommodating small-sized sciurids with “flying squirrel” dental pattern and demonstrating rather generalized, lightly-built cheek teeth with rugose enamel, underdeveloped secondary cusps (metaconule and paraconule), well-developed protolophule and mesostyle of P4–M2, and prominent metastylid, mesoconid, and ectomesolophid in p4–m3. This results in a plethora of fossil taxa formally attributed to *Hylopetes* and documented from both Europe and Asia throughout the early Miocene and Pleistocene. The problem is further complicated by the evident morphological similarities between *Hylopetes* and closely related flying squirrels. As shown by Bouwens and de Bruijn (1986), the living species of *Hylopetes* and *Petinomys* cannot be distinguished on the basis of dental morphology. Attempts to resolve the problem by splitting traditionally recognized *Hylopetes* into genera *Pliopetes*, *Neopetes*, and *Hylopetes* s.str. (Daxner-Höck, 2004) have been ignored by the majority of subsequent authors. The obvious limitation of such an attempt is that some living taxa confidently attributed to *Hylopetes* (e.g. *H. lepidus*) could easily fit the diagnosis of *Neopetes*.

Here, we recognize seven fossil species of *Hylopetes* s.l.: *H. hoeckarum* (Early to Late Miocene, Europe), *H. hungaricus* (Late Miocene — Late Pliocene, Europe), *H. macedoniensis* (Late Miocene, Europe and Anatolia); *H. auctor* (Late Miocene, China), *H. yani* (Early Pliocene, China), and *H. magistri* (Early Pliocene, Europe) (Kretzoi, 1959; Bouwens and de Bruijn, 1986; Qiu, 1991; de Bruijn, 1998; Reumer and van den Hoek Ostende, 2003; Qiu and Li, 2016). A recently described *H. bellus* (Qiu and Li, 2016, 2023) from the early Late Miocene of

Northwestern China is a small-sized sciurid that seems to possess a characteristic dental pattern of *Blackial/Tamiops* with slender cheek teeth, crenulated enamel, strong endoloph of M1–2, labially displaced posterior portions of M3 and m3, oblique (posterolabially directed) protoloph and metaloph of M1–2, and weak mesoconid and rudimentary trigonid basin of m1–2. Hence, we prefer to exclude this species from *Hylometes*, while still refraining from placing it in *Blackial/Tamiops*.

The specimens from Tagay described above represent a medium-sized species of *Hylometes* s.l., roughly equal in dimensions to *H. auctor*, *H. macedoniensis*, and *H. yani*, but smaller than *H. hoeckarum* and *H. magistri*, and larger than *H. hungaricus*. In overall morphology, they resemble most of the teeth of *H. (Pliometes) hungaricus* in having a strong protolophule, antecinus and sinus depressions on a distinctly rectangular M1–2. However, the enamel is not as wrinkled as in *H. hungaricus*. This character also distinguishes the form from Tagay and many extant members of the genus, including a morphologically similar *H. phayrei*. Given the limitations of the available materials, lack of critical tooth loci, and some ambiguity in the interpretation of morphological characters, the putative arrow-tailed flying squirrel from Tagay is only attributed to the genus *Hylometes* s.l. here. It is possible, however, that future discoveries of more complete material and larger sampling will necessitate the description of a new species.

Subfamily Xerinae Osborn, 1910

Tribe Marmotini Pocock, 1923

Genus *Miospermophilus* Black, 1963

Miospermophilus debruijni (Daxner-Höck et al., 2022b)

Fig. 4, 5

2022 *Spermophilinus debruijni* nov. spec., Daxner-Höck et al., 2022b; Fig. 7.

Material — GIN 1138/125, 127, left DP4; GIN 1138/96, 126, 192, right DP4; GIN 1138/67, 98, 99, 127, 137, 168, 191, left P4; GIN 1138/68, 97, right P4; GIN 1138/69–71, 73, 100, 102, 103, 104, 106, 108, 128, 130, 131, 133, 134, 138, 168–171, 173, 174, left M1–2; GIN 1138/72, 74, 101, 129, 132, 170, 193, 194, right M1–2; GIN 1138/107, 135, 136, left M3; GIN 1138/75, 76, 122, 199 right M3; GIN 1138/51, 139, 195, left dp4; GIN 1138/78, 79, 109, 150, 151, right dp4; GIN 1138/83, 110, 111, 140, 152, left p4; GIN 1138/53, 80–82, 153, 154, 196, right p4; GIN 1138/55, 57, 77, 84, 85, 87, 92, 114, 115, 144, 157, 158, 197, left m1; GIN 1138/54, 56, 141, 142, 155, 162, right m1; GIN 1138/59, 95, 116, 119, 120, 143, 159, 161, 163–165, 178, 190, left m2; GIN 1138/58, 61, 86, 94, 112, 113, 117, 118, 123, 156, 160, right m2; GIN 1138/63, 64, 66, 90, 121, 166, left m3; GIN 1138/62, 88, 89, 124, 198, and 200 right m3.

Description — Deciduous P4 is triangular in occlusal outline and almost equal in length and width (Table). The anterior and lingual sides of the crown are widely

Table. Measurements of *Miospermophilus debruijni*, Tagay (in mm)

	N	min	mean	max	SD	CV
DP4						
L	4	1.33	1.40	1.48	0.0687	4.9
W	4	1.38	1.40	1.42	0.0228	1.62
L/W	4	0.95	1.00	1.07	0.0527	5.28
P4						
L	10	1.36	1.47	1.56	0.0523	3.55
W	8	1.70	1.85	2.03	0.1049	5.66
L/W	8	0.73	0.80	0.85	0.0362	4.54
M1–2						
L	21	1.36	1.50	1.65	0.0162	4.95
W	19	1.71	1.87	2.03	0.0173	4.03
L/W	19	0.73	0.80	0.86	0.0082	4.48
M3						
L	7	1.83	1.90	1.97	0.0547	2.87
W	7	1.77	1.83	1.92	0.0545	2.98
L/W	7	1.00	1.04	1.11	0.0365	3.51
dp4						
L	5	1.18	1.26	1.42	0.0928	7.36
W	5	1.09	1.15	1.24	0.0928	5.77
L/W	5	1.01	1.09	1.16	0.0625	5.71
p4						
L	12	1.35	1.40	1.47	0.0382	2.72
W	11	1.20	1.28	1.43	0.0709	5.55
L/W	11	1.03	1.10	0.78	0.0457	4.16
m1						
L	14	1.38	1.50	1.70	0.0945	6.2956
W	14	1.56	1.75	1.90	0.1092	6.2536
L/W	14	0.79	0.86	0.93	0.0316	3.6711
m2						
L	23	1.50	1.61	1.81	0.0658	4.0938
W	23	1.80	1.93	2.11	0.0792	4.0987
L/W	23	0.78	0.83	0.92	0.0349	4.1925
m3						
L	9	1.78	2.01	1.91	0.0625	3.28
W	9	1.93	2.13	2.00	0.0570	2.85
L/W	9	0.91	1.01	0.95	0.0277	2.9

rounded; the posterior and lingual sides are flattened (Fig. 4A–D). The anterior lobe is vast and constitutes about 70% of the anterior side of the tooth. Lingually, the transition between the anterior lobe and the anterior face of the protocone is only barely defined by a shallow

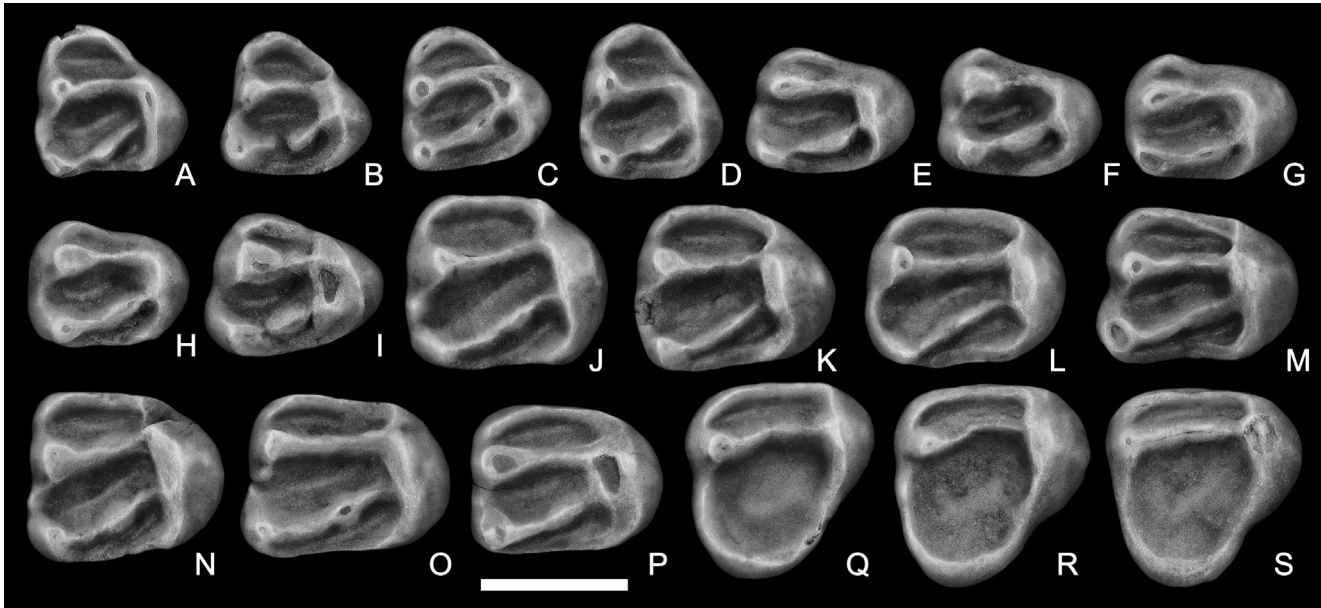


Fig. 4. *Miospermophilus debruijini* (Daxner-Höck et al., 2022b), upper cheek teeth, Tagay; A, DP4 (GIN 1138/126); B, DP4 (GIN 1138/167); C, DP4 (GIN 1138/96); D, DP4 (GIN 1138/125); E, P4 (GIN 1138/98); F, P4 (GIN 1138/168); G, P4 (GIN 1138/92); H, P4 (GIN 1138/137); J, M1-2 (GIN 1138/132); K, M1-2 (GIN 1138/131); L, M1-2 (GIN 1138/69); M, M1-2 (GIN 1138/131); N, M1-2 (GIN 1138/74); O, M1-2 (GIN 1138/70); P, M1-2 (GIN 1138/71); Q, M3 (GIN 1138/134); R, M3 (GIN 1138/135); S, M3 (GIN 1138/122); B, E, F, I, H, K–M, O–R — inverted. Scale bar equals 1 mm.

anterolingual incisure. As a result, the anterolingual edge of the crown is virtually straight. The anterior valley is rimmed by a well-developed anteroloph having a stronger labial and a somewhat weaker lingual arm. This is particularly the case of GIN 1138/125, which possesses a very thin and low lingual anteroloph. The anterocone is a gentle thickening on the anterior part of the labial anteroloph. The arm ends abruptly before reaching the anterior face of the paracone in all, except one tooth (GIN 1138/125), which has a thin labial arm of the loph enclosing the anterior valley laterally. The opposite, lingual side of the anterior valley remains open in three of the four DP4s. A sizeable anterostyle is visible in one specimen (GIN 1138/167; Fig. 4B). The protocone, endoloph, and hypocone form a longitudinal crest oriented nearly parallel to the labial side of the crown. The paracone and metacone are circular and pointed. The paracone and the anterior side of the protocone are connected by a complete and straight protoloph. The metaloph is slightly oblique and complete. GIN 1138/167 demonstrates an incomplete metaloph, interrupted at the contact between the labial and lingual halves of the ridge (Fig. 4B). This specimen is noticeable for a pointed metaconule, located approximately halfway between the protocone and metacone. In the remaining three DP4s the metaconule is present as a weak thickening of the metaloph. The central sinus is dammed by a well-developed premetacrista, bearing a well-defined mesostyle swelling. The posteroloph is a low, even, and thick ridge that thickens toward the hypocone. The tooth is three-rooted.

The P4 is an anteroposteriorly compressed and roundly rectangular in occlusal aspect (Table). The lin-

gual (protocone) side of the crown is fairly rounded (Fig. 4E–I). The posterior side is flat and the anterior one is slightly concave. The labial side of the crown varies in shape from gently convex to concave at the area of the sinus. The most characteristic feature of the tooth is a rudimentary anterior lobe. In four specimens (GIN 1138/68, GIN 1138/97, GIN 1138/127, GIN 1138/168) the lobe is confined to a small protrusion on the anterolabial side of the crown and devoid of the anteroloph (Fig. 4F). In (GIN 1138/67, GIN 1138/98, GIN 1138/137) the lobe is longer and dominated by a thin anteroloph that stretches along the anterior merge of the tooth (Fig. 4E), and in GIN 1138/137 reaches the anterior face of the protocone (Fig. 4I). Among the cusplets of the anterior valley, only the anterocone is discernible as a weak swelling on the foremost extent of the anteroloph. In unworn specimens, the protocone, endoloph, and hypocone are combined into a longitudinally or somewhat antero-laterally inclined ridge-like structure similar to that in the deciduous premolar. When worn, the protocone appears distinctly cusped, massive, and comma-shaped. The anterolabial end of the protocone continues with a strong and essentially straight protoloph. The labial end of the loph is fused with elliptical and anteroposteriorly compressed paracone. The metacone, albeit somewhat smaller and lower, is reminiscent of the paracone in overall shape. The metaloph is a complete ridge that arcs between the metacone and the posterior side of the protocone. The central portion of the metaloph bears a distinct swelling at this point that marks the presence of a weak metaconule. The labial arm of the metaloph in GIN 1138/127 is interrupted at the contact with the

metaconule. The posteroloph is crescent and featureless. It runs along the posterior wall of the crown to contact with the posterolingual base of the metacone. The posteroloph and protoloph merge with opposite ends of the lophate protocone and hypocone to form a U-shape crest. There is no distinct mesostyle or ectoloph in P4. The root system of the tooth is represented by a massive lingual root and about one and a half times thinner anterolabial and posterolabial roots.

The M1 and M2 are virtually identical in morphology and size and, therefore are lumped together here as one category, the M1–2 (Fig. 4J–P; Table). The crown is squared in occlusal view, with flattened anterior and posterior walls, a slightly concave labial wall, and a rounded lingual side. The posterior half of the crown is somewhat wider than the anterior one. The anterior valley is anteroposteriorly long, approximately equal to the central valley in length, and transversally wide, comprising 65–80% of the crown's width. A simple anteroloph runs along the anterior wall of the tooth from the anterolateral side of the paracone to the anterolingual side of the protocone. The connection between the latter and the loph is present in all M1–2s. The antesinus is a weak depression on the anterolingual corner of the crown. In seven specimens the anterior slope of the antesinus is defined by a knob-like anterostyle. The anterocone anterocone and paraconule are not discernible in any of the teeth. Laterally, the anterolabial sinus is enclosed in all, apart from one specimen (GIN 1138/74; Fig. 4N). The crown is dominated by a prominent protocone. As in the premolars, the cusp is lophate and merged with a rudimentary hypocone via a thick endoloph. In worn specimens the protoconid becomes distinctly cusped, showing a comma-shaped or elliptical wear facet. A straight and evenly smooth protoloph extends transversally from the anterolabial side of the protocone, ending labially with a triangular and pointed paracone. The metacone is somewhat lower and anteroposteriorly shorter than paracone. A slightly arched metaloph is an oblique ridge connecting the metacone and the posterolabial side of the protocone. The ridge is always complete, although demonstrating a faint constriction at the contact with the protocone. A small metaconule is observable in four of 27 specimens. In the remainder, the central path of the metaloph possesses a slight constriction, giving it a somewhat lobed appearance, but nothing that could be interpreted as a distinct metaconule. The ectoloph is present in nine M1s either as a complete but minute crest or a well-developed postparacrista. In five of these molars, the crest is further complicated by a tiny mesostyle. The hypocone is totally subsumed into an endoloph. The posteroloph starts from the posterior end of the endoloph, curves labially at the posterolingual corner of the crown, and extends labially to fade out gradually before reaching the metacone.

The M3 is nearly as long as its width, with a broad anterior part of M3 and a relatively narrow posterior valley, giving the crown a roughly triangular outline (Fig. 4Q–S; Table). In most specimens, the labial edge of the crown is straightened or slightly indented at the contact between the posterior lobe and the paracone. The opposite, lingual margin, is distinctly concave. The anterior lobe of M3 is similar to the same part of M2, but even less complex. The anterior valley is always closed both labially and lingually. None of the specimens possesses the parastyle and anterocone. A faint anterostyle is observable as a thickening of the lingual arm of the anteroloph, best seen in medium-worn teeth. The protocone is a tall, slightly mediolaterally compressed, and crescentic cusp, dominating the lingual half of the crown. The most prominent structure on its labial half is a pointed, conical paracone. The lingual extension of the paracone joins the anterior arm of the protocone to form a well-developed and complete protoloph that is slightly bowed anteriorly in most specimens, or nearly straight in GIN 1138/136. Due to the absence of metaloph, metacone, and metaconule, the central and posterior valleys are seamlessly fused to form a vast posterior basin covered by a smooth enamel. The basin is surrounded posteriorly and labially by a thin posteroloph with no recognizable cusps. Lingually, the posteroloph is continuous with a faint hypocone swelling that, in turn, contacts the posterior extent of the protocone via an obliquely oriented endoloph. The anterior side of the hypocone is accentuated in two of nine M3s by a sharp sinus. The tooth is three-rooted.

The dp4 is slightly smaller than its permanent replacement and has a more slender crown with a narrower anterior portion than the p4 (Table). Viewed occlusally, the dp4 crown is trapezoid or roundly triangular; the talonid is 16 to 28% wider than the trigonid (Fig. 5A–D). The trigonid consists of three main cusps: the metaconid, protoconid, and anteroconulid. Among them, the metaconid is the strongest cusp. It is about 25% taller and wider than the protoconid, and shifted more anteriorly, thus forming the entire anterolingual side of the trigonid. There is a well-developed trigonid basin that is only partially closed posteriorly in three of six specimens by a weak labial metalophid. The anteroconulid is a knob-like cuspid on the anterolabial edge of the trigonid. The cuspid is somewhat connected to the protoconid by a weak labial anterolophid. The lingual anterosinusid remains open in all dp4s. A straight ectolophid extends from the rear wall of the protoconid along the labial edge of the crown to meet the anterolingual side of the hypoconid. The ridge only slightly tapers towards the hypoconid and is devoid of the mesoconid. The sinus is simple, with no signs of ectostylid. The hypoconid is comparable in diameter with the protoconid and roundly triangular in the occlusal aspect. The pos-

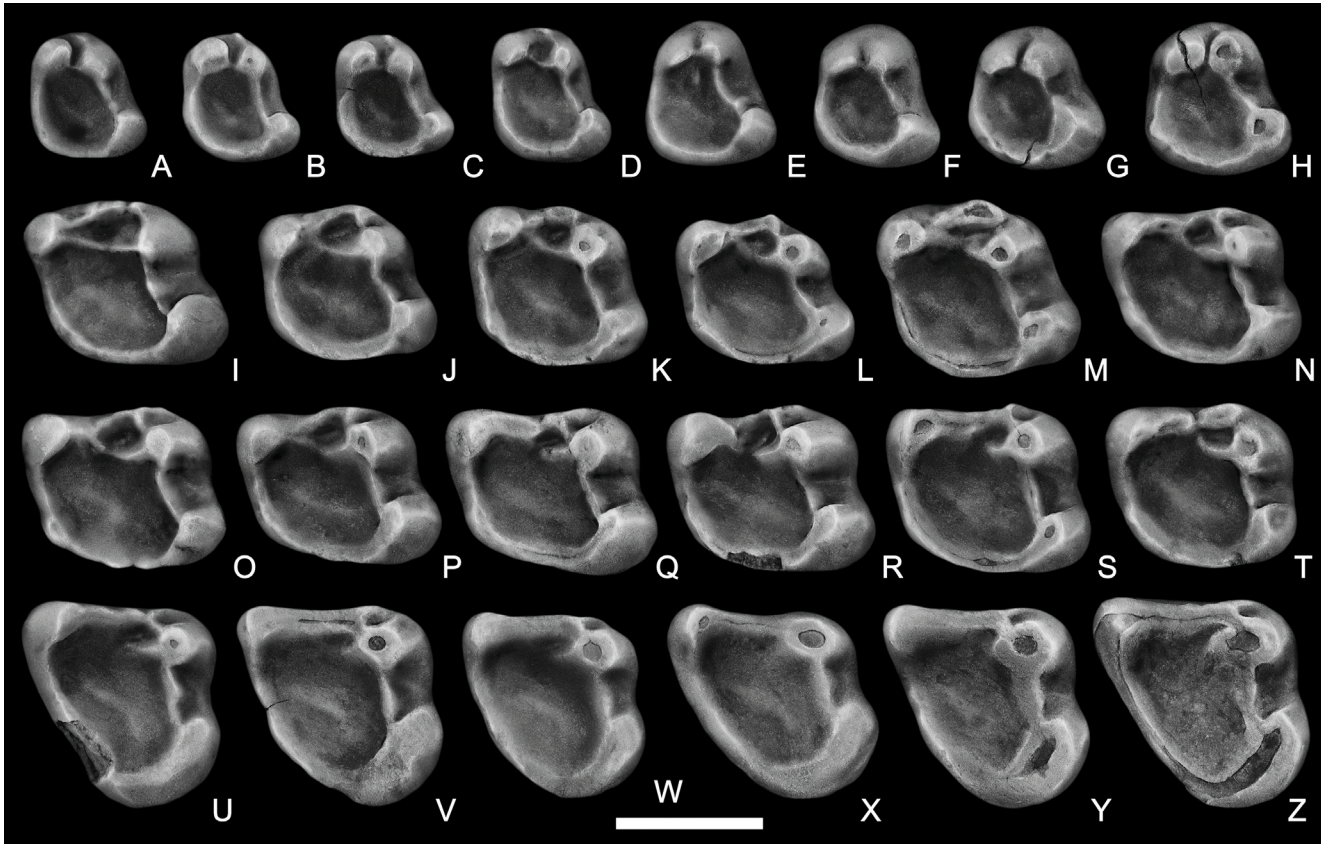


Fig. 5. *Miospermophilus debruijini*, lower cheek teeth, Tagay; A, dp4 (GIN 1138/79); B, dp4 (GIN 1138/151); C, dp4 (GIN 1138/150); D, dp4 (GIN 1138/195); E, p4 (GIN 1138/111); F, p4 (GIN 1138/80); G, p4 (GIN 1138/83); H, p4 (GIN 1138/140); I, m1 (GIN 1138/144); J, m1 (GIN 1138/54); K, m1 (GIN 1138/56); L, m1 (GIN 1138/155); M, m1 (GIN 1138/57); N, m2 (GIN 1138/117); O, m2 (GIN 1138/159); P, m2 (GIN 1138/112); Q, m2 (GIN 1138/119); R, m2 (GIN 1138/143); S, m2 (GIN 1138/118); T, m2 (GIN 1138/116); U, m3 (GIN 1138/89); V, m3 (GIN 1138/121); W, m3 (GIN 1138/198); X, m3 (GIN 1138/ 89); Y, m3 (GIN 1138/62); Z, m3 (GIN 1138/166). D, E, G–I, M, O, Q, R, T, V, Z — inverted. Scale bar equals 1 mm.

terolophid continues from the hypoconid to the posterolingual edge of the metaconid, enclosing the talonid basin. A fairly cuspsate entoconid is observable in three specimens; the rest demonstrate a barely discernible swelling of the posterolophid marking the presence of a rudimentary cusp. GIN 1138/79, GIN 1138/109, and GIN 1138/150 are noticeable for a weak hypoconulid, accentuated labially by a shallow postflexid depression (Fig. 5A, C). As typical for sciurids, the crown is supported by two divergent and widely spaced roots.

The p4 is more distinctly trapezoid in occlusal outline and more stout than the deciduous tooth, with a broader trigonid portion that is 18 to 35 % narrower than the talonid (Fig. 5E–H; Table). The anterior side of the crown is roundly convex, the lingual and posterior sides are flattened, and the lingual side is slightly concave. The metaconid and protoconid are large, tightly appressed, round in outline, and almost equal in size. The trigonid basin is a sharp slit-like depression between the protoconid and metaconid. In all specimens, the basin is opened both posteriorly and anteriorly. In GIN 1138/111 and GIN 1138/140 a faint anteroconulid is barely represented on the anterior face of the trigonid (Fig. 5E, H). The talonid basin is rounded, smooth, and enclosed labially,

posteriorly, and lingually by complete ectolophid and posterolophid, respectively. The ectolophid is low and mainly featureless straight ridge connecting the protoconid and the hypoconid. The hypoconid of p4 is proportionally larger than that of dp4, although is similar in the overall shape. A thin and complete posterolophid arises from the posterolingual part of the hypocone and runs along the talonid basin to contact the posterior part of the metaconid. The entoconid is weaker than the deciduous premolar. It thickens into a gentle swelling of the posterolophid defined by a small wear facet in five of twelve specimens. Neither the hypoconulid nor the lingual cusps, namely the mesostylid and metastylid, are present in p4. All teeth are two-rooted.

The m1 is substantially larger than p4, slightly anteroposteriorly compressed in occlusal view, with its trigonid width being slightly shorter than its talonid width (Fig. 5I–M; Table). The three main cusps are nearly equal in diameter. The metaconid is the tallest cusp, followed by the protoconid and hypoconid. The fourth principal cusp, the entoconid, is rudimentary and submerged into the posterolophid. The anterolophid forms the anterior margin of the tooth between the protoconid and metaconid. The labial half of the crest thickens

into a small anteroconulid defined by a teardrop-shaped wear facet. A thin labial arm of the protoconid forms a weak bridge connecting the protoconid with the anteroconulid. The anterolabial corner of the crown between the cusps is depressed by a narrow anterosinusid. The metaconid, represented by a thin lingual arm and a somewhat thicker labial arm is low but continuous from the protoconid to the metaconid, closing off a rounded and shallow trigonid basin. The talonid basin is a vast, featureless, and roughly rectangular depression. The hypoconid varies in occlusal outlines from triangular to nearly trapezoid. The ectolophid is straight and even throughout its length. A tiny swelling on the labial wall of the ectolophid seen in GIN 1138/114, GIN 1138/144, and GIN 1138/157 marks the presence of a rudimentary mesoconid (Fig. 5I). The posterolophid is a narrow ridge that arcs from the hypoconid to the entoconid to rim the posterior side of the talonid basin. The ectolophid is present in six of sixteen m1s. The metastylid and entoconid crests are seamlessly fused, so that the talonid basin remains enclosed lingually in all specimens.

The m2 is distinctly anteroposteriorly compressed, with a rudimentary posterolingual (entoconid) corner of the crown (Fig. 5N–T; Table). The talonid is slightly narrower than the trigonid; and the labial portion of the crown (across protoconid and hypoconid) is longer than the opposite, lingual side (across metaconid and entoconid). As in m1, the crown is dominated by the massive metaconid and lower protoconid and hypoconid; the entoconid is strongly reduced. The crown of m2 has a concave labial margin at the midline, an evenly concave anterior, and posterior and lingual margins that appear straightened to slightly convex. A weak, yet distinct anteroconulid is present on the terminal end of a prominent anterolophid. The anterosinusid is a deep slit separating the anteroconulid and the anterior wall of the protoconid. The slit terminates lingually approximately on the level with the lingual side of the protocone by a thin anterior arm of the cusp, and not its central part, as seen in most m1s. The metalophid is also substantially shorter than in m1 and represented exclusively by its labial arm that connects the midpoint of the anterolophid. This results in a very restricted, teardrop-shaped trigonid basin confined between the labial metalophid, lingual wall of the protoconid, and anterolophid. The ectolophid is a thin and straight ridge with a slightly thickened medial portion, which in five of twenty m2s forms a faint labial protrusion associated with a remnant of the mesoconid. The largest talonid cusp is the hypoconid, which is trapezoid to rectangular in occlusal outline and slightly anteroposteriorly compressed. A well-developed posterolophid forms the entire posterior wall of the crown. The entoconid is submerged into the posterolophid. A weak swelling of the entoconid is discernible in five teeth. GIN 1138/118 possesses a tiny metastylid sitting on a thin

metastylid crest (Fig. 5S). The latter is present in all teeth and forms the lingual rim of the talonid basin. The tooth has four roots of which the posterolingual (entoconid) root is the weakest, one and a half to two times shorter and thinner than the posterolabial root.

The m3 is the largest of the cheek teeth (Table). The talonid portion of the crown is only slightly narrower than the trigonid and noticeably shifted labially so that the angle between the anterior and labial sides of the crown is always obtuse (Fig. 5U–Z). The anterior half of the crown is reminiscent of that of m2, but unlike the more anterior molar, it has a weaker anterosinusid and anteroconulid, represented by a narrow labial anterolophid; stronger anterior arm of the protoconid and rudimentary metalophid. The latter is discernible in three of five m3s as a slight lingual protrusion of the protoconid. The talonid and trigonid basins are fused and smooth. The ectolophid is complete, and straight, but low. Its medial portion is always thickened, however, the only unambiguous indication of a mesoconid is a small swelling at the center of the ectolophid, seen in three specimens. A massive hypoconid continues lingually by a thick posterolophid. Running lingually the ridge curves anteriorly to form a weak entoconid swelling observable in four teeth. A thin entoconid crest descends the entoconid anteriorly, where it becomes confluent with a metaconid crest in all, except for one tooth (GIN 1138/200), which lacks the lingual crest but reveals a well-developed elliptical mesostylid. The root system of the tooth is represented by three constantly present roots: the massive posterolabial root, and weaker anterolingual and anterolabial roots. In five specimens these three roots are supplemented by a tiny fourth root located either between the posterolabial and anterolingual roots or partially fused with the posterolingual root in one specimen (GIN 1138/200).

Comparisons and comments — The sciurid community of Tagay is dominated by a small representative of the marmotine subtribe *Marmotina*, as suggested by a set of morphological characters including a weak entoconid of p4–m2, rudimentary metalophid of m2, and, most importantly, the lack of mesoconid in the lower cheek teeth. These characters place it apart from chipmunks (subtribe *Tamiina*, genera *Eutamias*, *Neotamias*, and *Tamias*) and rock squirrels (subtribe *Sciurotamiina*, genera *Csakvaromys*, *Palaesciurus*, *Protospermophilus*, and *Sciurotamias*) (Sinita, 2018; Sinita, Čermák, and Kryuchkova, 2022). Two Oligo-Miocene representatives of basal *Marmotina* have been documented and described from North America and Asia. Black (1963) erected *Miospermophilus* for small-sized ground squirrels that he placed in an intermediate position between sciurines and marmotines and viewed the genus as the most likely candidate for the ancestral stock of *Spermophilus* s.l. This assumption has been rigorously sup-

ported by morphology-based phylogenetic analysis of Marmotini placing *Miospermophilus* in the basalmost position within a monophyletic Marmotina clade (Sinitza, 2018). This analysis retrieved a sister taxon for *Miospermophilus*, the Asian latest Oligocene to Early Miocene genus *Plesiosciurus*. Both genera are remarkably similar and were recently proposed to be congeneric, based primarily on the reanalysis of their morphology and preliminary results of the examination of the specimens from Tagay (Sinitza and Delinschi, 2023).

Currently, the genus comprises five species: the type species, *M. bryanti*, late Early Miocene (Hemingfordian NALMA) to Middle Miocene (Barstovian NALMA) of Colorado and Nebraska (Wilson, 1960; Black, 1963; Korth and Evander, 2016); *M. wyomingensis*, late early Miocene (late Hemingfordian) of Wyoming (Black, 1963); *M. laveryi*, early Late Miocene (Clarendonian NALMA) of Oklahoma (Dalquest, Baskin, and Schultz, 1996); *M. sinensis*, Early Miocene (Shanwangian ALMA) of Eastern China (Qiu and Lin, 1986; Qiu, 2015) and late Oligocene to early Middle Miocene of Mongolia (Maret, Daxner-Höck, Badamgarav, and Göhlich, 2014); and *M. zhengi*, Early? Miocene of Eastern China (Qiu and Jin, 2016). The other occurrences of unidentified species of *Miospermophilus* have been reported from the late Oligocene to Middle Miocene of California, Florida, Nebraska, Nevada and South Dakota (Pratt and Morgan, 1989; Goodwin, 2008; Korth, 2009), making it both a geographically and temporarily widespread sciurid.

The specimens from Tagay represent a small-sized species of *Miospermophilus*. It is smaller than *M. laveryi*, *M. zhengi*, and *M. wyomingensis*, and roughly corresponds in size to small specimens of *M. sinensis* from Sihong (Qiu and Lin, 2005) and *M. bryanti* from Pawney Creek Formation (Wilson, 1960) and Observation Quarry locality (Black, 1963). In terms of dental morphology *M. bryanti* and *M. sinensis* are very similar and differ primarily by somewhat more reduced mesoconids in the latter, which could suggest its more crownward position in the evolutionary tree of marmotines relative to *M. bryanti*. All subsequent members of the genus, both Asian and North American, appear more derived in dental morphology and demonstrate larger metaconules and distinctly constricted metalophs. The specimens from Tagay referable to *Miospermophilus* belong to a very primitive representative of the genus, more basal than any other species known to date, as suggested by: 1. its small size; 2. rudimentary anterior lobe of P4 (this character, albeit shared by all species of *Miospermophilus*, seems to demonstrate an evolutionary trend towards a more expanded anterior lobe in geologically younger taxa); 3. weak to almost absent metaconules and complete metalophs of P4, M1, and M2; and 4. more frequent mesoconids and pronounced anterosinusids in the lower cheek teeth.

Daxner-Höck et al. (2022a) erected a new species of *Spermophilinus* (= *Csakvaromys*), *S. debruijni* on the basis of seven cheek teeth from Tagay (originally, Tagay-1). They distinguished “*S.*” *debruijni* from other species of *Csakvaromys* by the lack of hypocone, entoconid and secondary cusps(-ids), such as anteroconule, metaconule, paraconule, anteroconid, mesoconid, and mesostylid, and by a short P4 having a rudimentary anterior valley. These characters not only differ “*S.*” *debruijni* from all known species of the genus but clearly indicate its taxonomic distinction from *Csakvaromys*. The possession of a rudimentary anterior lobe of P4, and the lack of hypocone, entoconid, and mesoconid suggest its Marmotina affinities, so “*S.*” *debruijni* is reallocated to *Miospermophilus* here as *M. debruijni*.

Sciuridae incertae sedis

Genus *Blackia* Mein, 1970

Blackia cf. *miocaenica* Mein, 1970

Fig. 3D–F

Material — GIN 1138/105, left M1–2; GIN 1138/187, right m1; GIN 1138/186, left m2; GIN 1138/174, left m3.

Description — The M1–2 in occlusal outline is rectangular to rhomboidal (L–1.57, W–1.79 mm). A straight anterior wall and a concave posterior wall are roughly subparallel and the labial wall is obliquely oriented, with the metacone set labial to the paracone. The lingual wall of the crown is somewhat uneven and demonstrates the antesisinus and sinus depressions. The main cusps are pointed and the ridges are straight. A strong anteroloph extends along the entire anterior margin of the crown, joining the anterior arm of the protocone lingually. This junction is a sharp ridge oriented at approximately a right angle to the transversal anteroloph. The latter is devoid of any signs of the anterocone and anterostyle. The anterior valley is large but shallow. Labially, the valley is dammed by a longitudinal preparacrista. Both the protoloph and metaloph are straight, even, and connected to a pointed protocone. The paracone and metacone are conical and similar in size, with the former being somewhat more elevated. There is a pronounced ectoloph between the cusp, formed by the fusion of equally developed posparacrista and premetacrista. The point of the fusion is marked by a blunt, although laterally expanded mesostyle. A vast central valley is shallow. Its bottom gradually slopes laterally from the protocone to attain its greatest depth at a point posterolingual to the paracone. The posterior portion of the crown is rudimentary. The endoloph possesses a minute swelling at its posterior extent that represents the hypocone. A low posteroloph runs laterally from this swelling to fade out before contacting the posterolabially shifted metacone. The posteroloph is tightly appressed to the metaloph, leaving a very short and shallow posterior valley. The anterior and, especially, central valleys of the tooth are

filled with fine crenulations, partially obliterated by wear in GIN 1138/105.

The m1 is approximately rhomboidal in occlusal outline (L–1.02, W–1.14 mm; Fig. 3D). The trigonid is slightly narrower than the talonid. The metaconid and protoconid are well-spaced and rather pointed; the former is slightly larger, higher, and more anterior than the protoconid. The anterolophid is a moderately elevated ridge along the anterior margin of the tooth. The middle section of the ridge is swollen and somewhat deformed by extensive crenulations. Labially and lingually the anterolophid is connected to the anterior walls of the protoconid and metaconid respectively. The lateral end of the ridge is continued by a pronounced labial anterolophid that forms a deep anterosinusid. The metalophid appears to be low, obscured by crenulations, and recessed at its midlength. Similar to the trigonid cusps, the labial ones, the protoconid and the hypoconid, are well-spaced from each other by an anteroposteriorly expanded sinusid. The ectolophid is free from accessory structures and consists of two sections of different lengths: a shorter posteromedially oriented anterior portion adjacent to the posterior wall of the protoconid, and about two times longer, posterolaterally oriented posterior portion. Meeting each other at almost a straight angle, these sections form a characteristic L-shaped ectolophid, which completely dams the talonid basin labially. The entire bottom of a shallow talonid basin is covered with minute, albeit pronounced, lophules and cusplets. The structures of the lingual side of the crown are obscured by wear but appear to be represented by a weak metastylid crest and a low mesostylid separated from a weak entoconid by a lingual sinusid. The posterolophid is a rudimentary loph connecting the entoconid with the posterolingual corner of the hypoconid.

The m2 is similar to m1 but is slightly wider anteriorly, giving it an even more rhomboidal occlusal outline (L–1.19, W–1.45 mm; Fig. 3E). The other subtle difference is that the metalophid is less pronounced than in m1 and lacks a labial portion. The anterolophid, however, appears to be thicker than in the preceding molar. The crown is supported by two anteroposteriorly compressed and slightly alternate roots of similar size and morphology.

The m3 has a triangular crown with its talonid portion being shifted laterally relative to the trigonid (L–1.57, W–1.64 mm; Fig. 3F). The main cusps, except the entoconid, are pointed and set close to the edge of the occlusal surface. The metaconid is the taller cusp followed by the protoconid and hypoconid. The entoconid is reduced to a barely discernible elevated section of the posterolophid. The anterolophid is straight and proportionally shorter than in m1–2. The lateral end of the crest does not form either anteroconulid or labial extension and connects to the anterior wall of the protoconid

via the anterior arm of the cusp. The metalophid is absent. The ectolophid and related structures on the lateral side of the crown are reminiscent of those of m1–2. The only obvious difference is the posterior portion of the ectolophid that bends lingually in m3, giving the ridge an S-shaped appearance. The rounded posterior lobe of the crown is marked by a pointed hypoconid. The aforementioned structures define the anterior and lateral walls of a vast rectangular depression of the fused trigonid and talonid basins. The depression is filled with sinuous, irregular lophules extending from the margins of the basins toward their common center. Lingually, the depression is enclosed by a complete, narrow ridge that runs from the metaconid to the hypoconid. Apart from a weak entoconid swelling, there are no indications of stylar cusps or hypoconulid on the ridge.

Comparison and comments — The late Cenozoic fossil record of Holarctic reveals several forms of small-sized sciurids sharing a remarkably similar and distinct dental pattern characterized by a combination of: 1. the lightly-built cheek teeth with crenulated enamel; 2. underdeveloped cusps; 3. relatively large P3; 4. the P4 with transversally wide anterior valley; 5. the rectangular M1–2 with widened posterior part, vast central valley, strong ectoloph, posteromedially skewed metaloph and protoloph, and lacking the hypocone, secondarily cusps and lophules (anterolophule and protolophule); 6. lower cheek teeth with reduced number of roots (up to two in each tooth loci); 7. restricted trigonid basin of m2; 8. m1–m3 with constantly present anterosinusid, weak entoconid, a complete posterolophid confluent with metaconid crest, and a distinctly L-shaped ectolophid lacking a strong mesoconid; 9. M3 and m3 lack the mesoloph and entolophid, respectively. Depending on geography, these problematic sciurids have been attributed either to the European extinct “flying squirrel” *Blackia*, a living Asian callosciurine *Tamiops* (Qiu and Yan, 2005; Qiu and Lin, 2016), or the extinct North American “flying squirrel” *Sciurion* (Skwara, 1986). In his original description of *Blackia* Mein (1970) viewed it within the so-called “third group” of flying squirrels, together with *Aeromys*, *Hylopetes*, *Petinomys*, and *Pliopetes*. The petauristine affinities of *Blackia* have been criticized by Thorington, Schennum, Pappas, and Pitassy (2005); most of the subsequent authors, however; conservatively view the genus as a “flying squirrel”. The genus *Sciurion*, known by three species, *S. campestre*, *S. oligocaenicus*, and *S. xenokleitus* (Skwara, 1986; Bell, 2004) from the late Oligocene and Early Miocene of Cypress Hill Formation in Saskatchewan, Canada, was informally allied by Skwara (1986) with flying squirrels, because of crenulated enamel covering the basins of unworn cheek teeth. However, she declined to assign it formally to the petauristines, and allocated it only to the Sciuridae. We consider *Blackia* and *Sciurion* closely related, if not congeneric. They are taxa with unclear affinities

with any of the five currently recognized squirrel subfamilies, and we consider them as ‘Sciuridae incertae sedis’ until more informative material becomes available. Qiu and Yan (2005) and Qiu and Li (2016) described two new species of *Tamiops* from the Miocene of China. Although the *Tamiops* affinities for *T. asiaticus* from the late Early Miocene to early Middle Miocene Shanwang fossil site seem plausible, the second species, *T. minor* from the late Middle Miocene to early Late Miocene of Balunhalagen appears remarkably similar to *Blackia miocaenica* in size and dental morphology. These apparent similarities were also recognized by the authors, who noted (Qiu and Li, 2005: p. 540): “There is no doubt that if European *Blackia* had been found in China it would have been allocated to *Tamiops*, and vice versa.”

We are of the opinion that the only reliable dental structure distinguishing *Blackia* and the living species of *Tamiops* is the root systems of their lower cheek teeth. The type species of the genus *Blackia*, *B. miocaenica*, possesses two massive roots on m1, m2, and m3, formed by fused anterior and posterior root pairs. The root system of the same teeth loci in *Tamiops* (the character has been examined for *T. maritimus*, *T. mccllellandii*, and *T. swinhoei*) is represented by three roots: a free posterior pair and a fused anterior one. Unfortunately, the structure of roots has not been reported for putative extinct Asiatic striped squirrels *T. asiaticus* and *T. minor*. Luckily, the material from Tagay described above, albeit confined to four specimens, presents a nearly intact m2 preserving its root system. This tooth is distinctly two-rooted, and identical to *Blackia* in this condition.

Blackia is reported from an astonishing time interval spanning from the Early Miocene to the late Early Pliocene (Mein, 1970; Dahlmann, 2001; Daxner-Höck, 2004). Throughout this time interval of approximately 20 My, the genus remains surprisingly stable in dental morphology. As a result, most specialists recognize only two species of *Blackia*: the type species *B. miocaenica* and *B. woelfersheimensis*. The latter species is known primarily from the Pliocene of central Europe and according to the original diagnosis (Mein, 1970) differs from *B. miocaenica* by very minor details of dental morphology such as a more sub-rectangular P4 with reduced anterostyle (originally, parastyle), a well-developed ectoloph on upper cheek teeth, rudimentary anterosinusid of m1–2, and slightly larger size. Most of these morphological differences were not confirmed upon examination of material from Wölfersheim, thus the species status for *B. woelfersheimensis* (Dahlmann, 2001) cannot be confirmed. The specimens from Tagay are virtually identical in dental morphology with the type material of *B. miocaenica* from the type locality La Grive L (Mein, 1970), whereas the M1–2 is somewhat larger and m1 and m2 are shorter than reported for the species. Although these slight size differences are probably artifactual and

reflect differences in measuring techniques, we prefer to assign the Tagay specimens to *B. miocaenica* only tentatively because of their scarcity and obvious geographical disparity, with over 4000 km separating Tagay and the previously known easternmost occurrences of *Blackia*.

Discussion

The Tagay sciurid community among other contemporary assemblages of Eurasia and North America

Sciurids are reasonably common in the Early Neogene fossil record of Eastern Asia, where up to six taxa of squirrels are known to co-occur in one fossil site. The vast majority of these finds, however, are documented from the subtropics of China, whereas the fossil record of Neogene sciurids from high-latitude regions of Asia remains frustratingly poor. Fossil rodents from the Early Miocene Tagay fossil site on Lake Baikal were first reported about 65 years ago (Kitainik and Ivaniev, 1958). Subsequent work has greatly expanded our knowledge of the small mammal fauna from this site, which remains the northernmost occurrence of Early Neogene terrestrial vertebrates in Asia.

The sciurid community of Tagay is represented by at least five taxa including bushy-tailed (*Sciurus* cf. *lii* and *Sciurus* sp.), flying (*Hylomyscus* sp.), ground squirrels (*Miospermophilus debruijini*), and a sciurid with unidentified subfamilial position (*Blackia* cf. *miocaenica*). Such a diversity places it among the taxonomically richest Sciuridae-bearing local faunas of Eurasia. Regarding taxic abundance, however, the sciurid fauna of Tagay is dominated by ground squirrels, in which *Miospermophilus* constitute 91.5% of the sciurid fossils. This assemblage echoes some Early Miocene (Shanwangian ALMA) Chinese faunas such as Sihong and Shanwang (Qiu, 2015; Qiu and Yan, 2005). Both include the bushy-tailed squirrel *Sciurus lii* and a species of *Miospermophilus*. However, the absence of medium-sized putative flying squirrels *Shuanggouia* and *Parapetaurista* in Tagay clearly differs it from Sihong. In contrast, the sciurid assemblage of Shanwang appears more similar to that of Tagay. Apart from the presence of *Miospermophilus* in Shanwang, the similarity is further accentuated by the appearance of two tree squirrels, *Sciurus lii* and *Oriensciurus linquensis*, and *Tamiops asiaticus*, a species perhaps closely related to *Blackia*, found in Tagay.

The Early Miocene sciurid fossil record of Europe is probably the most complete known globally. Recently documented Early Miocene small mammal communities from Anatolia contain taxa previously associated with Central European faunas and seem to be devoid of any non-European endemics (Bosma, de Bruijn, and Wessels, 2018). This implies a wider geographical range of early

Miocene “European” sciurid communities that, presumably, expanded far beyond present-day Europe. Some sciurid taxa present in Tagay, however, are unknown in Europe before the late Miocene. Among them are members of the genus *Sciurus* and representatives of *Marmotina*, which made their first appearance in Europe at the latest Miocene and early Late Miocene, respectively (Colombero and Carnevale, 2016; Sinita, 2018; Sinita and Delinschi, 2023). Two other sciurids reported in Tagay, the Eurasian flying squirrel *Hylopetes* and Holarctically distributed *Blackia* unite it with European early Miocene assemblages.

Three of the four genus-level sciurid taxa from the Tagay are notable for showing affinities to taxa outside Eurasia. Of these, the marmotine *Miospermophilus*, is otherwise known from the late Oligocene to the Middle Miocene of North America. Although *M. debruijni* is considered morphologically the most primitive species of the genus, its presence in Tagay is linked with a wave of Nearctic migrant taxa crossing the Bering land bridge in the late Oligocene and Early Miocene. The Nearctic origin for *Sciurus* and *Blackia*, however, is doubtful. Both genera are reported from North America, but they are either represented by very scanty remains or their first appearance in the Asian fossil record predates that in the Nearctic (Emry, Korth, and Bell, 2005; Goodwin, 2008). The flying squirrels of the genus *Hylopetes* remain undocumented from North America. Apart from this Eurasian sciurid, whose northernmost distribution in Asia is evidenced by the specimens described herein, the sciurid community from Tagay can be interpreted as an Eastern Asian Early Miocene community in the migratory corridor between Eurasia and North America.

Ecology of the Tagay sciurid community

Previous researchers reconstructed various paleoenvironments for Tagay primarily as closed, forested habitats with a temperate climate (Daxner-Höck et al., 2022a). As mentioned above, the squirrel community of Tagay is dominated by a marmotine ground squirrel. Despite their formal status, many living marmotine ground squirrels remain ecologically generalized and are known to occupy mixed and forested biomes, which is, for instance, the case of many living chipmunks, and *Sciurotamias* rock squirrels (Thorington, Koprowski, Steele, and Whatton, 2012). It should be noted, however, that these generalized marmotines are not typical tree-dwellers, whereas an arboreal lifestyle, similar to that in living bush-tailed squirrels, is suggested for some extinct *Sciurotamiina* (Sinita, Čermák, and Kryuchkova, 2022). Members of the genus *Miospermophilus* have never been an object for direct paleoecological analyses. Given their dental morphology and the position in the phylogenetic tree of ground squirrels, between the chipmunks and basal *Marmotina* (genera *Sinotamias* and *Ammospermophilus*), one can as-

sume that *Miospermophilus* was a generalized semi-arboreal form, similar in habit and lifestyle to the present-day chipmunks. The remaining sciurid taxa from Tagay are more informative as environmental indicators.

The flying squirrel *Hylopetes* sp. is remarkably similar in dental pattern to the living arrow-tailed flying squirrel *H. lepidus*, a typical small- to medium-sized pteromyine preferring closed-canopy, dense forests. Conventionally attributed to the flying squirrels, *Blackia* is considered here a *Sciuridae* incertae sedis. Although the dental characters purportedly allying it with pteromyines are phylogenetically insignificant, the extensive enamel crenulation of *Blackia* is shared by living leaf-eating tree and flying squirrels. Given the absence or rarity of *Blackia* in typical subtropical and tropical open biomes-dominated local faunas, it is tempting to hypothesize that members of the genus were specialized tree-dwellers, possibly similar to some present-day small-sized callosciurines.

Sciurus is a typical tree-dwelling squirrel and as such testifies to the presence of forested areas. In Tagay the large-sized *Sciurus* cf. *lii* co-occurs with a small, yet unidentified, species. Such combinations have not been reported for fossil sciurid communities, whereas similar co-occurrences are not exceptional among the living bush-tailed squirrels of Central and South America, where up to three small- and large-sized sympatric species can occupy the same geographical area (Thorington et al., 2012). The co-occurrence of *Sciurus* cf. *lii* and *Sciurus* sp. in Tagay may suggest a niche partitioning between the taxa and a high productivity of arboreal biomes allowing them to co-exist. As such, we reconstruct the sciurid assemblage from Tagay as an element of arboreal- and semi-arboreal ecosystems that existed in the temperate climate of Eastern Siberia in late Early Miocene, between ca. 17 and 16 Mya.

Acknowledgments

We thank the reviewers (Joshua X. Samuels and an anonymous reviewer) for reading the paper and making useful suggestions. This study is in accordance with the plan of scientific research of the Ural Federal University, Università Roma Tre, and the Geological Institute of the Russian Academy of Sciences.

Members of the Tagay project are acknowledged for the efficient team efforts which brought the fossil material described in this paper.

References

- Bell, S. D. 2004. Aplodontid, Sciurid, Castorid, Zapodid, and Geomyoid rodents of the Rodent hill locality, Cypress Hills formation, Southwest Saskatchewan. Thesis. 192 pp. University of Saskatchewan, Saskatoon.
- Black, C. C. 1963. Miocene rodents from the Thomas Farm local fauna, Florida. *Bulletin of the Museum of Comparative Zoology* 128:483–501.
- Bosma, A., de Bruijn, H., and Wessels, W. 2019. Early and middle Miocene *Sciuridae* (Mammalia, Rodentia) from Anatolia, Turkey. *Journal of Vertebrate Paleontology* 38(6):e1537281. <https://doi.org/10.1080/02724634.2018.1537281>

- Bouwens, P. and de Bruijn, H. 1986. The flying Squirrels *Hypopetes* and *Petinomys* and their fossil record. *Proceedings of the Koninklijke Nederlandse Akademie van Wetenschappen B* 89(2):113–123.
- Bowdich, T. E. 1821. An analysis of the natural classifications of Mammalia for the use of students and travellers. J. Smith, Paris, 115 pp.
- Brandt, J. F. 1855. Beiträge zur nähern Kenntniss der Säugethiere Russlands. *Mémoires de l'Académie Impériale des Sciences de Saint-Petersbourg* 6:1–365.
- Colombero, S. and Carnevale, G. 2016. Late Miocene (Turolian, MN13) squirrels from Moncucco Torinese, NW Italy. *Comptes Rendus Palevol* 15:515–526. <https://doi.org/10.1016/j.crpv.2015.09.021>
- Dahlmann, T. 2001. Die Kleinsäuger der unter-pliozänen Fundstelle Wölfersheim in der Wetterau (Mammalia: Lipotyphla, Chiroptera, Rodentia). *Courier Forschungsinstitut Senckenberg* 227:1–129.
- Dalquest, W. W., Baskin, J. A., and Schultz, G. E. 1996. Fossil mammals from a late Miocene (Clarendonian) site in Beaver County, Oklahoma; pp. 107–137 in H. H. Genoways, R. J. Baker (eds.). *Contributions in Mammalogy: A Memorial Volume Honoring Dr. J. Knox Jones, Jr.* Museum of Texas Technical University, Lubbock.
- Daxner-Höck, G. 2004. Flying squirrels (Pteromyiinae, Mammalia) from the Upper Miocene of Austria. *Annalen des Naturhistorischen Museums Wien* 106(A):387–423.
- Daxner-Höck, G., Böhme, M., and Kossler, A. 2013. New data on Miocene biostratigraphy and paleoclimatology of Olkhon Island (Lake Baikal, Siberia); pp. 508–519 in X. Wang, L. J. Flynn, and M. Fortelius (eds.). *Fossil Mammals of Asia: Neogene Biostratigraphy and Chronology*. Columbia University Press, New York. <https://doi.org/10.7312/columbia/9780231150125.003.0022>
- Daxner-Höck, G., Mörs, T., Kazansky, A. Yu., Matasova, G. G., Ivanova V. I., Shchetnikov, A. A., Filinov, I. A., Voyta, L. L., and Erbajeva, M. A. 2022a. A synthesis of fauna, palaeoenvironments and stratigraphy of the Miocene Tagay locality (Olkhon Island, Lake Baikal, Eastern Siberia). *Palaeobiodiversity and Palaeoenvironments* 102(4):969–983. <https://doi.org/10.1007/s12549-022-00558-8>
- Daxner-Höck, G., Mörs, T., Filinov, I., Shchetnikov, A., and Erbajeva, M. A. 2022b. Geology and lithology of the Tagay-1 section at Olkhon Island (Lake Baikal, Eastern Siberia), and description of Aplodontidae, Mylagaulidae and Sciuridae (Rodentia, Mammalia). *Palaeobiodiversity and Palaeoenvironments* 102(4):843–857. <https://doi.org/10.1007/s12549-022-00548-w>
- de Bruijn, H. 1998. Vertebrates from the Early Miocene lignite deposits of the opencast mine Oberdorf (Western Styrian Basin, Austria): 6. Rodentia 1 (Mammalia). *Annalen des Naturhistorischen Museums in Wien* 99A:99–137.
- Emry, R. J., Korth, W. W., and Bell, M. A. 2005. A tree squirrel (Rodentia, Sciuridae, Sciurini) from the Late Miocene (Clarendonian) of Nevada. *Journal of Vertebrate Paleontology* 25:228–235. [https://doi.org/10.1671/0272-4634\(2005\)025\[0228:ATSRSS\]2.0.CO;2](https://doi.org/10.1671/0272-4634(2005)025[0228:ATSRSS]2.0.CO;2)
- Fabre, P. H., Hautier, L., Dimitrov, D., and Douzery, E. J. 2012. A glimpse on the pattern of rodent diversification: A phylogenetic approach. *BMC Evolutionary Biology* 12:1–19. <https://doi.org/10.1186/1471-2148-12-88>
- Fischer, G. 1817. *Adversaria zoologica, fasciculus primus. Mémoires de la Société impériale des naturalistes de Moscou* 5:357–446.
- Goodwin, T. H. 2008. Sciuridae; pp. 355–376 in C. M. Janis, G. F. Gunnell, M. D. Uhen (eds.). *Evolution of Tertiary Mammals of North America. Vol. 2: Small mammals, xenarthrans, and marine mammals. Evolution of Tertiary Mammals of North America*. Cambridge University Press, Cambridge. <https://doi.org/10.1017/CBO9780511541438.022>
- Kazansky, A. Yu., Shchetnikov, A. A., Matasova, G. G., Filinov I. A., Erbajeva, M. A., Daxner-Höck, G., and Mörs, T. 2022. Palaeomagnetic data from the late Cenozoic Tagay section (Olkhon Island, Baikal region, Eastern Siberia). *Palaeobiodiversity and Palaeoenvironments* 102(4):943–967. <https://doi.org/10.1007/s12549-022-00559-7>
- Kitainik, A. F. and Ivaniev, L. N. 1958. Note on Tertiary deposits of Olkhon Island on Lake Baikal. *Zapiski Irkutsk. Oblast. Kraeved. Muz.* 55–60. (In Russian)
- Klementiev, A. M. and Sizov, A. V. 2015. New record of anchitherium (*Anchitherium aurelianense*) in the Miocene of Eastern Siberia, Russia. *Russian Journal of Theriology* 14(2):133–143. <https://doi.org/10.15298/rusjtheriol.14.2.02>
- Korth, W. 2009. Mammals from the Blue Ash local fauna (Late Oligocene), South Dakota. Rodentia, part 3: Family Sciuridae. *Paludicola* 7(2):47–60.
- Korth, W. and Evander R. L. 2016. Lipotyphla, Chiroptera, Lagomorpha, and Rodentia (Mammalia) from Observation Quarry, Earliest Barstovian (Miocene), Dawes County, Nebraska. *Annals of Carnegie Museum* 83(3):219–254. <https://doi.org/10.2992/007.083.0301>
- Kretzoi, M., 1959. Insectivoren, Nagetiere und Lagomorphen der jüngpliozänen Fauna von Csarnóta im Villányer Gebirge (Südungarn). *Vertebrata Hungarica* 1(2):237–246.
- Linnaeus, C. 1758. *Systema Naturae per Regna Tria Naturae, Secundum Classes, Ordines, Genera, Species, cum Characteribus, Differentiis, Synonymis, Locis. Tomus I. Editio decima, reformata.* 824 pp. Laurentii Salvii, Stockholm. <https://doi.org/10.5962/bhl.title.542>
- Logatchev, N. A., Lomonosova, T. K., and Klimanova, V. M. 1964. The Cenozoic deposits of the Irkutsk amphitheatre. 196 pp. Nauka Publ., Moscow. (In Russian)
- Maridet, O., Daxner-Höck, G., Badamgarav, D., and Göhlich, U. B. 2014. New discoveries of sciurids (Rodentia, Mammalia) from the Valley of Lakes (Central Mongolia). *Annalen des Naturhistorischen Museums Wien, Serie A* 116:271–291.
- Mein, P. 1970. Les Sciuropteres (Mammalia, Rodentia) Neogènes d'Europe occidentale. *Geobios* 3(3):7–77. [https://doi.org/10.1016/S0016-6995\(70\)80001-8](https://doi.org/10.1016/S0016-6995(70)80001-8)
- Osborn, H. F. 1910. *The age of Mammals in Europe, Asia and North America.* 635 pp. Macmillan Co., New York. <https://doi.org/10.5962/bhl.title.102077>
- Pocock, R. I. 1923. The classification of the Sciuridae. *Proceedings of the Zoological Society of London* 93(2):209–246. <https://doi.org/10.1111/j.1096-3642.1923.tb02184.x>
- Pokatilov, A. G. 2012. Stratigraphy of Cenozoic of Eurasia (paleontological grounding). 304 pp. Irkutsk State University Press, Irkutsk. (In Russian)
- Pratt, A. E. and Morgan, G. S. 1989. New Sciuridae (Mammalia: Rodentia) from the Early Miocene Thomas Farm Local Fauna, Florida. *Journal of Vertebrate Paleontology* 9(1):89–100. <https://doi.org/10.1080/02724634.1989.1001741>
- Qiu, Z.-D. 1991. The Neogene mammalian faunas of Ertemte and Harr Obo in Inner Mongolia (Nei Mongol), China. 8. Sciuridae (Rodentia). *Senckenbergiana Lethaea* 71(3):223–255.
- Qiu, Z.-D. 2015. Revision and supplementary note on Miocene sciurid fauna of Sihong, China. *Vertebrata PalAsiatica* 53(3):219–237.
- Qiu, Z.-D. and Jin, C. Z. 2016. Sciurid remains from the Late Cenozoic fissure-fillings of Fanchang, Anhui, China. *Vertebrata PalAsiatica* 54(4):286–301.

- Qiu, Z.-D. and Li, Q. 2016. Neogene Rodents from Central Nei Mongol, China. *Palaeontologia Sinica, New Series C* 30:1–684.
- Qiu, Z.-D. and Li, Q. 2023. Miocene squirrels from Linxia Basin, Gansu, China; paleoenvironmental and palaeoecological implications. *Palaeogeography Palaeoclimatology Palaeoecology* 619(1/2):111530. <https://doi.org/10.1016/j.palaeo.2023.111530>
- Qiu, Z.-D. and Lin, Y. P. 1986. The Aragonian vertebrate fauna of Xiacaowan, Jiangsu. 5. Sciuridae (Rodentia, Mammalia). *Vertebrata Palasiatica* 24(3):191–205.
- Qiu, Z.-D. and Yan, C. L. 2005. New sciurids from the Miocene Shanwang Formation, Linqiu, Shandong. *Vertebrata Palasiatica* 43(3):194–207.
- Rage, J.-C. and Danilov, I. G. 2008. A new Miocene fauna of snakes from eastern Siberia, Russia. Was the snake fauna largely homogenous in Eurasia during the Miocene? *Comptes Rendus Palevol* 7:383–390. <https://doi.org/10.1016/j.crvp.2008.05.004>
- Rasmussen, N. L. and Thorington R. W., Jr. 2008. Morphological differentiation among three species of flying squirrels (genus: *Hylopetes*) from Southeast Asia. *Journal of Mammalogy* 89:1296–1305. <https://doi.org/10.1644/07-MAMM-A-303.1>
- Reumer, J. W. F. and van den Hoek Ostende, L. W. 2003. Petauristidae and Sciuridae (Mammalia, Rodentia) from Tegelen, Zuurland, and the Maasvlakte (The Netherlands). *Deinsea* 10:455–467.
- Sinitsa, M. V. 2018. Phylogenetic position of *Sinotamias* and the early evolution of Marmotini (Rodentia, Sciuridae, Xerinae). *Journal of Vertebrate Paleontology* e1419251:1–24. <https://doi.org/10.1080/02724634.2017.1419251>
- Sinitsa, M. V., Čermák, S., and Kryuchkova, L. Y. 2022. Cranial Anatomy of *Csakvaromys bredai* (Rodentia, Sciuridae, Xerinae) and Implications for Ground Squirrel Evolution and Systematics. *Journal of Mammalian Evolution* 29:149–189. <https://doi.org/10.1007/s10914-021-09561-w>
- Sinitsa, M. V. and Delinschi, A. 2023. A revision of *Sinotamias* (Rodentia, Sciuridae, Xerinae) from eastern Europe, with a discussion of the evolutionary history of the genus. *Historical Biology* 35(10):1917–1934. <https://doi.org/10.1080/08912963.2022.2127096>
- Sinitsa, M. V. and Pogodina, N. V. 2019. The evolution of early *Spermophilus* in eastern Europe and the antiquity of the Old World ground squirrels. *Acta Palaeontologica Polonica* 64(3):643–667. <https://doi.org/10.4202/app.00605.2019>
- Sizov, A. V. and Klementiev, A. M. 2015. Geology and taphonomy of Tagay locality of early Miocene vertebrate fauna; pp. 206–218 in E. A. Lipnina, I. M. Berdnikov (eds.). Eurasia in the Cenozoic. Stratigraphy, paleoecology, cultures. No. 4. Irkutsk State University Press, Irkutsk. (In Russian)
- Sizov, A. V., Klementiev, A. M., and Pierre-Olivier, A. 2023. An Early Miocene skeleton of *Brachydiceratherium* Lavocat, 1951 (Mammalia, Perissodactyla) from the Baikal area, Russia, and a revised phylogeny of Eurasian teleoceratines. *bioRxiv* <https://doi.org/10.1101/2022.07.06.498987>
- Skwara, T. 1986. A new “flying squirrel” (Rodentia: Sciuridae) from the Early Miocene of southwestern Saskatchewan. *Journal of Vertebrate Paleontology* 6(3):290–294. <https://doi.org/10.1080/02724634.1986.10011625>
- Sotnikova, M. V., Klementiev, A. M., Sizov, A. V., and Tesakov, A. S. 2021. New species of *Ballusia* Ginsburg and Morales, 1998 (Ursidae, Carnivora) from Miocene of Eastern Siberia, Russia. *Historical Biology* 33(4):486–497. <https://doi.org/10.1080/08912963.2019.1637864>
- Steppan, S. J., Storz, B. L., and Hofmann, R. S. 2004. Nuclear DNA phylogeny of the squirrels (Mammalia: Rodentia) and the evolution of arboreality from c-myc and RAG1. *Molecular Phylogenetics and Evolution* 30:703–719.
- Sulimski, A., 1964. Pliocene Lagomorpha and Rodentia from Węże 1 (Poland). *Acta Paleontologica Polonica* 9(2):149–244.
- Syromyatnikova, E. V. 2016. Anurans of the Tagay locality (Baikal Lake, Russia; Miocene): Bombinatoridae, Hylidae, and Ranidae. *Russian Journal of Herpetology* 23(2):145–157. <https://doi.org/10.30906/1026-2296-2016-23-2-145-157>
- Tesakov, A. S. and Lopatin, A. V. 2015. First record of Mylagaulid rodents (Rodentia, Mammalia) from the Miocene of Eastern Siberia (Olkhon Island, Baikal Lake, Irkutsk Region, Russia). *Doklady Biological Sciences* 460:23–26. <https://doi.org/10.1134/S0012496615010032>
- Thomas, O. 1908. The genera and subgenera of the Sciuropterus group, with descriptions of three new species. *Annals and Magazine of Natural History Series* 8:1–8. <https://doi.org/10.1080/00222930808692350>
- Thorington, R. W., Jr. and Hoffmann, R. S. 2005. Family Sciuridae; pp. 754–818 in D. E. Wilson and D. M. Reeder (eds.). Mammal species of the world. A taxonomic and geographic reference. 3rd ed. Johns Hopkins University Press, Baltimore.
- Thorington, R. W., Jr., Pitassy, D., and Jansa, S. A. 2002. Phylogenies of flying squirrels (Pteromyinae). *Journal of Mammalian Evolution* 9(1/2):99–135. <https://doi.org/10.1023/A:1021335912016>
- Thorington, R. W., Jr., Musante, A. L., Anderson, C. G., and Darrow, K. 1996. Validity of three genera of flying squirrels: *Eoglaucomys*, *Glaucumys*, and *Hylopetes*. *Journal of Mammalogy* 77(1):69–83. <https://doi.org/10.2307/1382710>
- Thorington, R. W., Jr., Schennum, C. E., Pappas, L. A., and Pitassy, D. 2005. The difficulties of identifying flying squirrels (Sciuridae: Pteromyini) in the fossil record. *Journal of Vertebrate Paleontology* 25:950–961. [https://doi.org/10.1671/0272-4634\(2005\)025\[0950:TDOIFS\]2.0.CO;2](https://doi.org/10.1671/0272-4634(2005)025[0950:TDOIFS]2.0.CO;2)
- Thorington, R. W. Jr., Koprowski, J. L., Steele, M. A., and Whatton, J. F. 2012. Squirrels of the world. pp. 459. Johns Hopkins University Press, Baltimore.
- Vislobokova, I. A. 1994. The Lower Miocene artiodactyls of Tagay Bay, Olkhon Island, Lake Baikal (Russia). *Palaeovertebrata* 23:177–197.
- Vislobokova, I. A. 2004. New species of *Orygotherium* (Palaeomyricidae, Ruminantia) from the Early and Late Miocene of Eurasia. *Annalen des Naturhistorischen Museums Wien* 106A:371–385.
- Volkova, N. V. 2020. The first fossil barbet (Aves, Ramphastidae) from Siberia. *Journal of Ornithology* 161:325–332. <https://doi.org/10.1007/s10336-019-01719-x>
- Volkova, N. V. and Zelenkov, N. V. 2018. A Scansorial Passerine Bird (Passeriformes, Certhioidea) from the Uppermost Lower Miocene of Eastern Siberia. *Paleontological Journal* 52(1):58–65. <https://doi.org/10.1134/S0031030118010148>
- van de Weerd, A. 1976. Rodent faunas of the Mio-Pliocene continental sediments of the Teruel-Alfambra region, Spain. *Utrecht micropaleontological bulletins, Special publication* 2:1–218.
- Wilson, R. W. 1960. Early Miocene rodents and insectivores from Colorado. *University of Kansas paleontological contributions. Vertebrata* 7:1–93.
- Zelenkov, N. V. 2016. The first fossil parrot (Aves, Psittaciformes) from Siberia and its implications for the historical biogeography of Psittaciformes. *Biology Letters* 12:20160717. <https://doi.org/10.1098/rsbl.2016.0717>